



UvA-DARE (Digital Academic Repository)

Moulting black holes

Bena, I.; Chowdhury, B.D.; de Boer, J.; El -Showk, S.; Shigemori, M.

DOI

[10.1007/JHEP03\(2012\)094](https://doi.org/10.1007/JHEP03(2012)094)

Publication date

2012

Document Version

Final published version

Published in

The Journal of High Energy Physics

[Link to publication](#)

Citation for published version (APA):

Bena, I., Chowdhury, B. D., de Boer, J., El -Showk, S., & Shigemori, M. (2012). Moulting black holes. *The Journal of High Energy Physics*, 2012, 094.
[https://doi.org/10.1007/JHEP03\(2012\)094](https://doi.org/10.1007/JHEP03(2012)094)

General rights

It is not permitted to download or to forward/distribute the text or part of it without the consent of the author(s) and/or copyright holder(s), other than for strictly personal, individual use, unless the work is under an open content license (like Creative Commons).

Disclaimer/Complaints regulations

If you believe that digital publication of certain material infringes any of your rights or (privacy) interests, please let the Library know, stating your reasons. In case of a legitimate complaint, the Library will make the material inaccessible and/or remove it from the website. Please Ask the Library: <https://uba.uva.nl/en/contact>, or a letter to: Library of the University of Amsterdam, Secretariat, Singel 425, 1012 WP Amsterdam, The Netherlands. You will be contacted as soon as possible.

Moulting Black Holes

Iosif Bena,¹ Borun D. Chowdhury,² Jan de Boer,² Sheer El-Showk¹ and Masaki Shigemori³

¹*Institut de Physique Théorique,*

CEA Saclay, CNRS URA 2306, F-91191 Gif-sur-Yvette, France

²*Institute for Theoretical Physics, University of Amsterdam,*

Science Park 904, Postbus 94485, 1090 GL Amsterdam, The Netherlands

³*Kobayashi-Maskawa Institute for the Origin of Particles and the Universe, Nagoya University, Nagoya 464-8602, Japan*

ABSTRACT: We find a family of novel supersymmetric phases of the D1-D5 CFT, which in certain ranges of charges have more entropy than all known ensembles. We also find bulk BPS configurations that exist in the same range of parameters as these phases, and have more entropy than a BMPV black hole; they can be thought of as coming from a BMPV black hole shedding a “hair” condensate outside of the horizon. The entropy of the bulk configurations is smaller than that of the CFT phases, which indicates that some of the CFT states are lifted at strong coupling. Neither the bulk nor the boundary phases are captured by the elliptic genus, which makes the coincidence of the phase boundaries particularly remarkable. Our configurations are supersymmetric, have non-Cardy-like entropy, and are the first instance of a black hole entropy enigma with a controlled CFT dual. Furthermore, contrary to common lore, these objects exist in a region of parameter space (between the “cosmic censorship bound” and the “unitarity bound”) where no black holes were thought to exist.

KEYWORDS: Black Holes in String Theory, AdS-CFT Correspondence

ARXIV EPRINT: [1108.0411](https://arxiv.org/abs/1108.0411)

Contents

1	Introduction and summary	1
2	CFT analysis	5
2.1	D1-D5 CFT	6
2.2	The enigmatic phase	7
2.2.1	The BMPV phase	8
2.2.2	The maximally-spinning state	8
2.2.3	The enigmatic phase	9
2.3	Numerical evaluation of partition function	11
2.3.1	BPS partition function and elliptic genera on single copy of $K3$ and T^4	12
2.3.2	BPS partition function and elliptic genera on $\text{Sym}^N(K3)$ and $\text{Sym}^N(T^4)$	14
2.3.3	Numerical evaluation of partition functions and elliptic genera	16
3	Supergravity analysis	18
3.1	Multi-centered Solutions in IIA/M-theory	18
3.1.1	Entropy, Angular momentum and CTCs	19
3.1.2	Gauge symmetries and “Spectral Flow”	20
3.1.3	T-dualizing to the IIB frame	21
3.1.4	$\text{AdS}_3 \times \text{S}^3$ and the AdS/CFT Dictionary	22
3.1.5	A Note on Signs	23
3.2	Two-centered Solutions in $\text{AdS}_3 \times \text{S}^3$	24
3.2.1	Stability and Smoothness	24
3.2.2	Spectral Flow in the Bulk	26
3.2.3	Spectral Flowing to BMPV plus Supertube	26
3.3	The BMPV plus Supertube System	28
3.3.1	Spectral Window	29
3.3.2	Entropy Maximization of a BMPV Black Hole Surrounded by a Supertube	30
3.3.3	New Phases in Supergravity	32
4	Discussion	34
4.1	A Supersymmetric Gregory-Laflamme Instability	35
4.2	The New Phases in the Canonical Ensemble	37
4.3	Future Directions	38
A	The Decoupling Limit	40
B	Spectral Flow	42
C	Stability analysis of two-center solution with one smooth center	42

D Why the “enigmatic states” do not contribute to the elliptic genus	44
E Units and conventions	45

1 Introduction and summary

The past few years have seen a great interest in the hair of black holes in anti-de Sitter (AdS) spacetimes. In AdS gravity coupled to other fields such as gauge fields and charged scalar fields, specifying the mass and charge of the configuration does not necessarily determine a unique black hole solution. Instead, one sometimes finds infinitely many solutions describing bound states of multiple black holes, or black holes surrounded by a condensate of other fields which is often referred to as “hair”.¹ For non-extremal black holes the existence of condensates, or hair, can be thought of as a thermodynamic instability for a charged black hole to emit one or several of its charges; in certain regimes this can *increase* the entropy of a black hole and thus it is entropically favorable for the black hole to reduce its charge by shedding charged hair outside the horizon.

For example, [1–7] found that a Reissner-Nordstrom black brane in AdS Maxwell gravity with a charged scalar (in bottom-up settings or embedded in string theory) is unstable against forming a charged scalar condensate outside its horizon and breaking the U(1) symmetry, and related this to the superconducting phase transition in the boundary field theory. As a different example embeddable in string theory, [8] studied a small R -charged black hole in $AdS_5 \times S^5$. They found that the black hole is unstable against forming an R -charged scalar condensate around it and constructed the endpoint configuration perturbatively when the charge is small.

Another example of this instability is the so-called entropy enigma [9, 10]: certain two-center BPS black hole configurations can have larger entropy than a single-center solution with the same asymptotic charges. Since for some charge choice one of these centers can uplift in five dimensions to a smooth geometry with flux, these particular enigmas can be thought of as black holes with hair around them. In [11], the entropy enigma was investigated in the context of the AdS/CFT correspondence by embedding it in $AdS_3 \times S^2$. It was found that this phenomenon occurs in the non-Cardy regime of the boundary CFT, where the entropy can deviate from the one naively expected from the Cardy formula. However, a complete CFT understanding of the entropy enigma has not been reached yet because of the limited knowledge on the dual MSW CFT [12, 13].

The purpose of this paper is to study the phase diagram² of the three-charge BPS black hole in five dimensions, and to determine the existence of new phases that contain

¹If one wants to reserve the word “hair” for genuine microstates of a black hole, then it is probably better to call the condensate a “halo”, because this configuration is better thought of as a bound state of a black hole and the condensate outside the horizon. However, we will use the word “hair” because this is a commonly used terminology in the literature.

²Unless stated otherwise, the word phase in this paper will refer to a microcanonical phase.

black holes with hair that have dominant entropy in certain regimes of parameters. For large angular momentum the BPS states we find can be thought of as the endpoints of a “thermodynamic” instability of a rotating D1-D5-P BPS black hole in $AdS_3 \times S^3$, and we identify these endpoint configurations both in the bulk and the boundary. Unlike previous enigma examples, our system has the advantage of being well-understood on both sides of holography.

More concretely, if N_p is the momentum charge along the S^1 direction of AdS_3 and J_L, J_R are the angular momenta³ in S^3 , then the left-moving energy L_0 of the dual D1-D5 CFT is equal to N_p (up to a constant shift) and the CFT R -charges are $J_{L,R}$. Now, let us consider a *microcanonical* ensemble specified by given fixed values of $N_p > 0$ and J_L (J_R is left unfixed), and ask what is the entropy of the ensemble. In the Cardy regime

$$N_p - J_L^2/4N \gg N, \tag{1.1}$$

where $c = 6N$ is the central charge, the Cardy formula and the spectral flow symmetry of the CFT give the entropy:

$$S_{\text{Cardy}} = 2\pi \sqrt{NN_p - J_L^2/4}. \tag{1.2}$$

In the bulk this corresponds to a single-center BPS black hole — the BMPV black hole [14], whose Bekenstein-Hawking entropy nicely reproduces the Cardy entropy (1.2). Although the Cardy formula is valid only in the region (1.1), the bulk BMPV black hole exists for any value of N_p larger than the bound $N_p = J_L^2/4N$.⁴ Furthermore, one can identify the CFT phase dual to the bulk BMPV black hole and show that this CFT phase (known as the “long string” sector) also exists all the way down to the cosmic censorship bound and that its entropy is always equal to (1.2) in the large N limit. Based on this, the phase diagram of the D1-D5 system has been thought to be the one shown in figure 1; above the cosmic censorship bound, the system is in the BMPV black hole phase while, below the bound, the system is in the phase of a gas of supergravity particles.

However, in the parameter region outside (1.1), namely in the *non-Cardy regime*, the Cardy formula (1.2) is no longer valid and there is no guarantee that the BMPV black hole phase is thermodynamically dominant. We will analyze in detail the possible phases both in the CFT and in the bulk, both analytically and numerically, and find *new phases* that for the same charges are thermodynamically dominant over other known phases in the non-Cardy regime. In the bulk, the new phase corresponds to a black hole surrounded by a supertube, or to a black ring. We can interpret both bulk solutions as resulting from the moulting or hair-shedding of the BMPV black hole. In one configuration the hair is a supertube, and in the other one the hair is a Gibbons-Hawking or Taub-NUT center (corresponding to a D6 brane in four dimensions) whose shedding changes the topology of the black hole horizon and transforms it into a black ring. As a result, the phase diagram shown in figure 1 is significantly modified in the non-Cardy regime.

³Our conventions are such that $J_{L,R}$ are integers.

⁴This bound is oftentimes called the “cosmic censorship bound” (e.g., ref. [15]), and we follow this terminology. Strictly speaking, this bound should instead be called the “chronological censorship bound”

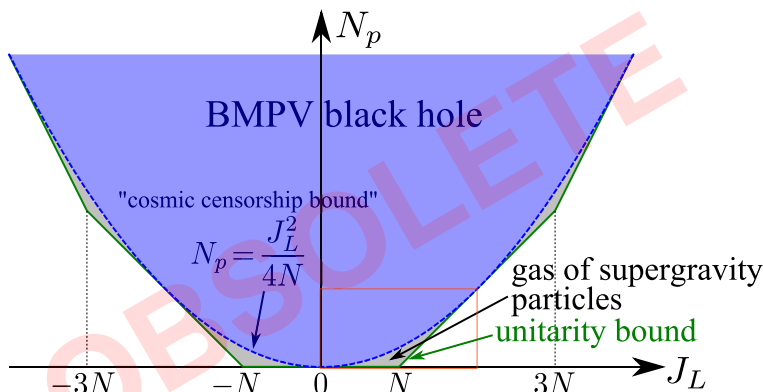


Figure 1. The “standard lore” but incorrect phase diagram of the D1-D5 system. Above the blue dotted parabola $N_p = J_L^2/4N$ (the cosmic censorship bound) is the BMPV black hole phase (light blue), while below the parabola is the phase of a gas of supergravity particles (gray). The range of N_p, J_L is bounded from below by the unitarity bound (green solid polygon).

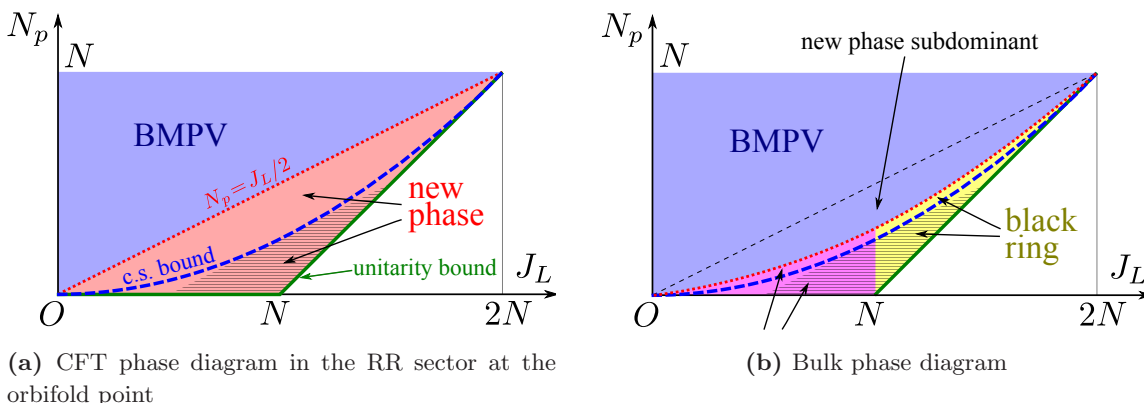


Figure 2. The updated, correct phase diagram of the D1-D5 system for the CFT and bulk (schematic, not to scale). The parameter range corresponds to the red rectangle in figure 1. The abbreviation “c.s. bound” refers to the cosmic censorship bound $N_p = J_L^2/4N$. For further explanations, see the text.

The CFT phase diagram is shown in figure 2a. If we start in the BMPV phase (light blue) with some large value of N_p and decrease N_p , then at $N_p = J_L/2$ (red dotted line) a new phase (light red region) becomes available before we reach the cosmic censorship bound (thick blue dashed curve). As soon as it becomes available, this new phase entropically dominates over the BMPV phase. As we further decrease N_p , the BMPV phase disappears at the cosmic censorship bound $N_p = J_L^2/4N$ (blue dashed line) while the new phase continues to exist and is dominant all the way down to the unitarity bound (green solid line). Below the cosmic censorship bound, the phase of a gas of supergravity particles is subdominant and not realized thermodynamically.

because, below this bound, the single-center black hole solution develops closed timelike curves outside the horizon but not a naked singularity.

The bulk phase diagram shown in figure 2b is somewhat similar, but there are some distinctive differences. As we start from the BMPV phase and lower N_p , a new phase appears at $N_p = J_L/2$, but has less entropy than the BMPV black hole until we further decrease N_p and reach the red dotted curve in figure 2b. After that, the new phase is dominant until the BMPV black hole disappears at the cosmic censorship bound (thin blue dashed curve). Below that, the new phase is dominant all the way down to the unitarity bound. Furthermore, for $J_L < N$, the new phase is a BMPV black hole with a hair of smooth geometry around it (light pink), while for $J_L > N$ it is a black ring (light yellow). On the $J_L = N$ line, these two configurations are entropically degenerate but remain distinct configurations.

Although in figure 2 we have shown only a small region of parameters N_p and J_L , by the spectral flow symmetry of the bulk and of the boundary, the new phase exists in all “wedges” below the cosmic censorship bound shown in figure 1 (see also figure 6).

The entropy of the CFT new phase is *larger* than that of the bulk new phase. Because the CFT computation was done in the free limit (at the orbifold point), this implies that, as we increase the coupling, some of the states that constitute the new phase in the CFT get lifted and disappear by the time we reach the gravity point. However, this lifting is quite moderate, and does not change the power of N that enters in the entropy formula, but only its prefactor; the new phases both in the CFT and the bulk are black hole states having an entropy of order $\mathcal{O}(N)$.

The fact that we have black holes below the cosmic censorship bound is intriguing for the following reason. In [16, 17], it was shown that the (modified) elliptic genus computed in CFT and the one computed in supergravity agree exactly for⁵

$$N_p \leq \frac{J_L}{2} - \frac{N-1}{4}. \tag{1.3}$$

This parameter range is shown in figure 2 as horizontally hatched regions and is below the cosmic censorship bound. One expects that, once one turns on coupling, all states that are not protected will lift, and all that remain at strong coupling are the states captured by the elliptic genus. In [16, 17], the elliptic genus was correctly reproduced in supergravity by counting particles, without including any black hole states. This appears to imply that in the region (1.3) the only thing that exist in the bulk are supergravity particles and there are no black hole states. This was the reason why the phase diagram was thought to be as shown in figure 1. On the contrary, in the current paper we find black hole (and ring) states in supergravity even in the region (1.3). This means that there are many states which are not protected and are thus not captured by the elliptic genus but nevertheless do not lift.⁶ This might be suggesting the existence of a new index capturing these states.

⁵In [16, 17] the relevant inequality was given in terms of NS sector quantities as $L_0^{NS} \leq \frac{N+1}{4}$. Here this has been translated into the R sector.

⁶In $d = 4, \mathcal{N} = 4$ theories, it has been argued [18] that multi-center solutions are not captured by the supersymmetry index unless each center preserves 1/2 supersymmetry. Our multi-center solution is made of a 1/4-BPS center and a 1/2-BPS center and thus is not captured by the supersymmetry index by the general argument of ref. [18].

It is possible that such an index is related to the “new moonshine” [19] on the hidden underlying symmetry of K3 surfaces.

The original motivation for the current study was to find the microscopic description of supersymmetric black rings [20–23] in the D1-D5 CFT.⁷ A CFT understanding of black rings and their dipole charges [28–31] is of much interest in its own right and may help us identify the boundary description of the family of smooth supergravity solutions found in [26, 27]. In [24], a possible microscopic description of supersymmetric black rings in the D1-D5 CFT was proposed but it was based on a phenomenological assumption, and hence not entirely satisfactory. Here, we made attempts to make progress in this direction by asking what is the most entropic configuration for given charges N_p, J_L . The new phase on the CFT side has already been reported in [32], and in the current paper we are reporting progress on the bulk side based on recent developments. It is interesting that the most entropic configuration is indeed a black ring in a certain parameter region. We hope to come back to the microscopics of black rings in near future.

It was noted in [9] that certain configurations of multi-center black rings can have entropy larger than a single-center black hole with the same values of charges and angular momenta. However, to our knowledge, no systematic search for the maximum entropy configuration of multi-center black holes/rings has been done, and such configurations have never been investigated in the context of the AdS/CFT correspondence.⁸

The plan of the rest of the paper is as follows. In section 2, after reviewing some necessary background material, we study the phase diagram of the D1-D5 CFT. We find a new phase that has more entropy than the BMPV phase, and give a physically-intuitive picture for this. Then, we confirm the existence of the new phase more rigorously by numerically evaluating the CFT partition function. In section 3, we explore the phase diagram of the D1-D5 system in the dual supergravity description. We perform a thorough analysis of two-center solutions and find black hole and ring configurations that have more entropy than a single-center BMPV black hole in a certain region of parameters. Section 4 is devoted to the discussion of the results and future directions. In the appendices, we present technical details and further clarifications on the subjects discussed in the main text.

2 CFT analysis

In this section we study the possible phases of the D1-D5 CFT, for given momentum and angular momentum charges. For large values of these charges (in the Cardy regime), the Cardy formula predicts the entropy of the system which is known to be reproduced by the entropy of the BMPV black hole in the bulk. However, outside the Cardy regime, there

⁷By a microscopic description we mean a description in the UV CFT, corresponding to the asymptotic AdS₃ region at infinity. Near the horizon of a supersymmetric black ring, there is another AdS₃ region which corresponds to an IR CFT. The IR CFT description of supersymmetric black rings was discussed in [24, 25]. However, the IR CFT does not capture many interesting dynamical features of the D1-D5 system, such as dipole charges, multi-center solutions and the family of smooth geometries [26, 27], and thus is not of interest in the present paper.

⁸The configurations found in [9] are not in the regime of parameters discussed in the current paper. Their configurations have $N_p \sim \sqrt{N}$ while we are interested in $N_p \sim N$.

is no formula for the entropy of general CFTs. In the D1-D5 CFT, however, the explicit orbifold construction of the CFT allows us to make an educated guess on the phase outside the Cardy regime and its entropy formula, which we will confirm by computer analysis. We will find that, in a certain regime of parameter space, a new phase appears and entropically dominates over the BMPV phase.

2.1 D1-D5 CFT

In this subsection we give a quick review of the D1-D5 CFT. For a more detailed review, see for example [33].

Consider type IIB string theory on $S^1 \times M^4$ with N_1 D1-branes wrapping S^1 and N_5 D5-branes wrapping $S^1 \times M^4$, where $M^4 = T^4$ or $K3$. We take the size of M^4 to be string scale. The Higgs branch of this system flows in the IR to an $\mathcal{N} = (4, 4)$ SCFT whose target space is a resolution of the symmetric product orbifold $\mathcal{M} = (M^4)^N / S_N \equiv \text{Sym}^N(M^4)$, where S_N is the permutation group of order N and $N = N_1 N_5$ ($N = N_1 N_5 + 1$) for $M^4 = T^4$ (for $M^4 = K3$). The orbifold \mathcal{M} is called the “orbifold point” in the space of CFTs and the theory is easy to analyze at that point.

The CFT is dual to type IIB string theory on $AdS_3 \times S^3 \times M^4$. To have a large weakly-coupled AdS_3 , N must be large and the CFT must be deformed far from the orbifold point by certain marginal deformations (for recent work see [34–36]). In this work we will consider a new phase at the orbifold point and look for it at the supergravity point.

For presentation purposes, we will henceforth take $M^4 = T^4$, but much of the discussion goes through also for $M^4 = K3$. In particular, the existence of the new phase does not depend on whether $M^4 = T^4$ or $K3$ because it is constructed using structures common to both.

The theory has an $SU(2)_L \times SU(2)_R$ R -symmetry which originates from the $SO(4)$ rotational symmetry transverse to the D1-D5 system. There is another $SU(2)_1 \times SU(2)_2$ global symmetry which is broken by the toroidal compactification but can be used to classify states. We label the charges under these symmetries as $\alpha, \dot{\alpha}$ and A, \dot{A} respectively. At the orbifold point each copy of the CFT has four left-moving fermions $\psi^{\alpha A}$, four left-moving bosons $\partial X^{A\dot{A}}$, four right-moving fermions $\psi^{\dot{\alpha} A}$ and four right-moving bosons $\bar{\partial} X^{A\dot{A}}$. In addition the CFT has twist fields σ_n which cyclically permute $n \leq N$ copies of the CFT on a single T^4 . One can think of these twist fields as creating winding sectors in the D1-D5 worldsheet with winding over different copies of the T^4 .

The D1-D5 CFT is in the Ramond-Ramond sector because of asymptotic flatness and supersymmetry. Elementary bosonic twist fields (without any bosonic or fermionic excitations) are charged under $SU(2)_L \times SU(2)_R$ *viz.* $\sigma_n^{\alpha\dot{\alpha}}$ or under $SU(2)_1 \times SU(2)_2$ *viz.* σ_n^{AB} while elementary fermionic twist fields are charged under $SU(2)_L \times SU(2)_1$ *viz.* $\sigma_n^{\alpha A}$ or $SU(2)_R \times SU(2)_2$ *viz.* $\sigma_n^{\dot{\alpha} A}$. A general Ramond sector ground state is made up of these bosonic and fermionic twist fields with the total twist $\sum n = N$ as

$$|gr, gr\rangle = \prod_{n, \alpha, \dot{\alpha}, A, \dot{A}} (\sigma_n^{\alpha\dot{\alpha}})^{N_{n, \alpha\dot{\alpha}}} (\sigma_n^{AB})^{N_{n, AB}} (\sigma_n^{\alpha A})^{N_{n, \alpha A}} (\sigma_n^{\dot{\alpha} A})^{N_{n, \dot{\alpha} A}},$$

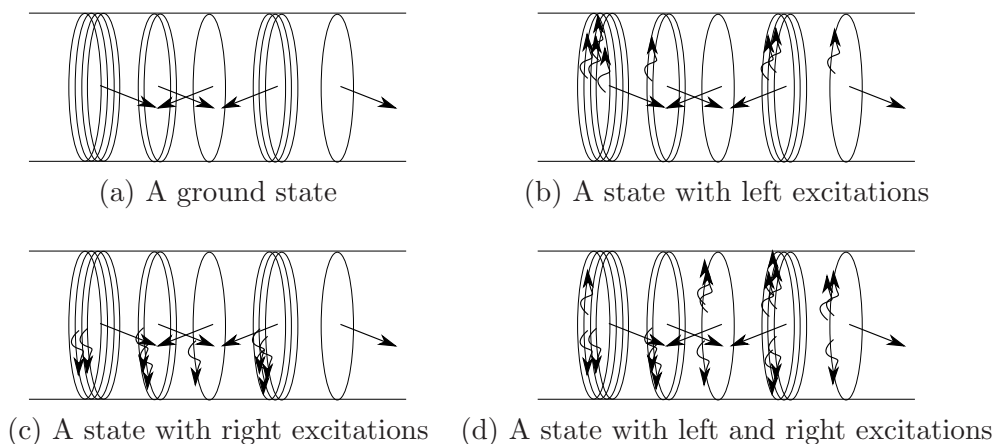


Figure 3. Various states in the Ramond sector of the D1-D5 CFT.

$$\sum_{n,\alpha,\dot{\alpha},A,\dot{A}} n(N_{n,\alpha\dot{\alpha}} + N_{n,AB} + N_{n,\alpha A} + N_{n,\dot{\alpha}A}) = N, \tag{2.1}$$

$$N_{n,\alpha\dot{\alpha}} = N_{n,AB} = 0, 1, 2, \dots, \quad N_{n,\alpha A} = N_{n,\dot{\alpha}A} = 0, 1.$$

A general Ramond sector state is made of left- and right-moving excitations on the Ramond ground states

$$|ex, gr\rangle, \quad |gr, ex\rangle, \quad |ex, ex\rangle \tag{2.2}$$

where “*ex*” means acting on Ramond ground states “*gr*” by the bosonic and fermionic modes. In figure 3 we diagrammatically represent a Ramond ground state with no excitations, left excitations only, right excitations only, and both. The arrows represent different *R*-charges of elementary twists.

The states of the CFT are characterized by their left and right dimension (L_0 and \bar{L}_0) and *R*-charges (J_L and J_R). In our conventions, $J_{L,R}$, the third components of the $SU(2)_{L,R}$ generators $\vec{J}_{L,R}$ are integers. The Ramond sector ground states all have the same dimension $L_0 = \bar{L}_0 = \frac{N}{4}$. An excited state has dimension greater than that of the ground state and any additional dimension is related to the left- and right-moving momentum along the branes by

$$N_p = L_0 - \frac{N}{4}, \quad \bar{N}_p = \bar{L}_0 - \frac{N}{4} \tag{2.3}$$

The relation between the momentum and dimension is not so straightforward in the NS sector as different twist sectors have different dimensions.

The CFT also has an outer automorphism called “spectral flow” [37]. Spectral flow by odd units maps states from NS to R sector and vice versa whereas spectral flow by even units maps states to states in the same sector. Under spectral flow by α units we have

$$L'_0 = L_0 + \frac{1}{2}\alpha J_L + \frac{1}{4}\alpha^2 N, \quad J'_L = J_L + \alpha N. \tag{2.4}$$

2.2 The enigmatic phase

In this subsection, we will first describe two phases in CFT at the orbifold point which are dual in the bulk to the BMPV black hole and to the maximally-spinning smooth

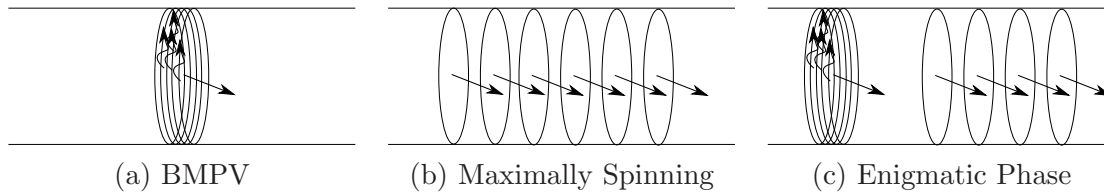


Figure 4. Three phases at the orbifold point of the D1-D5 CFT.

solution found by Balasubramanian, Keski-Vakkuri, Ross and one of the authors, and by Maldacena and Maoz [38, 39]. We will then explicitly construct the new phase, which we will call the enigmatic phase, in CFT by combining properties of the BMPV and the maximally-spinning phases. This will become clear as we proceed. We will then put this on a more rigorous footing by identifying the enigmatic phase in the BPS partition function of the CFT. We will also show that the elliptic genus fails to capture the enigmatic phase.

Our construction will be at the orbifold point of the CFT. Since the elliptic genus fails to capture the enigmatic phase, it is logically possible that this phase gets lifted once we move away from the orbifold point of the CFT moduli space by turning on deformation and go to the supergravity point. We will explore the possibility of an enigmatic phase on the gravity side in the next section.

2.2.1 The BMPV phase

The BMPV black hole [14] has $U(1)_L \times SU(2)_R$ symmetry and has an entropy

$$S_{\text{BMPV}} = 2\pi\sqrt{NN_p - J_L^2/4}. \quad (2.5)$$

Black holes have entropy and thus their CFT duals are ensembles of states. The dual to BMPV black holes consists of an ensemble of thermal excitations on the left-moving sector on a long string

$$(ex_L)\sigma_N^{++}. \quad (2.6)$$

The $SU(2)_L$ charge is carried by left-moving fermions. This phase is shown in a diagrammatic way in figure 4(a).

The subleading corrections to the above picture come from $O(1)$ winding in short strings.

When the charges are large so that we are in the Cardy regime $N_p - J_L^2/4N \gg N$, the Cardy formula (and the spectral flow symmetry) yields the same entropy as the Bekenstein-Hawking entropy of the black hole (2.5). Thus, in the Cardy regime, we have a nice matching of the CFT and the bulk.

2.2.2 The maximally-spinning state

Refs. [38, 39] found a family of smooth solutions with $U(1)_L \times U(1)_R$ symmetry that have no horizon and thus no entropy. Their CFT dual states can be uniquely determined: they have all the winding in single twists and their R-charges are in the largest multiplet:

$$(\sigma_1^{++})^N. \quad (2.7)$$

The phase is shown diagrammatically in figure 4(b).

This state has the largest possible value of J_L among the ground states, namely $J_L = N$. Among other possible ground states with $J_L = N$ are

$$(\sigma_1^{++})^{N-j}(\sigma_1^{-+})^j, \quad j = 0, 1, \dots, N. \quad (2.8)$$

These form an $SU(2)_R$ multiplet with $|\vec{J}_R| = N$.

2.2.3 The enigmatic phase

In the above, we discussed the BMPV phase which dominates at large momenta and the maximally-spinning state which has no momentum but very large angular momentum. Now let us consider combining these two, namely an ensemble of states where there is one long string and a condensate of short strings, and ask what is the entropy maximizing ensemble with given N_p, J_L (we assume $J_L > 0$ without loss of generality).

All the excitations are carried by the long string (fractionation ensures this is dominant [40]). Let l be the number of short strings. Thus the long string has winding $N - l$. The short strings are aligned with the left-moving angular momentum of the long strings so have $J_L = l$, and symmetrization ensure that the short strings form an $SU(2)_R$ multiplet with $|\vec{J}_R| = l$ just as in (2.8). Thus this phase has R-symmetry broken down to $U(1)_L \times U(1)_R$. This phase is shown in figure 4(c).

The entropy of this “enigmatic” phase comes from the long string sector which is the same as that in the BMPV phase albeit with different winding number and angular momentum

$$S_{\text{enigma},l} = 2\pi\sqrt{(N-l)N_p - \frac{1}{4}(J_L - l)^2}. \quad (2.9)$$

Maximizing this entropy with respect to l , the winding in the short strings, we get the optimal number of short strings to be⁹

$$l = J_L - 2N_p \quad (2.10)$$

and the entropy for this is

$$S_{\text{enigma}} = 2\pi\sqrt{N_p(N_p + N - J_L)}. \quad (2.11)$$

The enigmatic phase exists in the region where the square of the entropy is positive and the number of short strings is greater than zero, namely

$$N_p > 0, \quad N_p + N - J_L > 0, \quad J_L - 2N_p > 0. \quad (2.12)$$

This means that $N_p \sim J_L \sim N$ and therefore this phase exists *outside* the Cardy regime. In addition the new phase is charged under $SU(2)_R$ with

$$|\vec{J}_R| = J_L - 2N_p. \quad (2.13)$$

⁹Splitting the system into two parts and choosing the way of splitting so that the entropy is maximized is reminiscent of the procedure taken in [8] where the system is split into a “non-interacting mix” of a black hole and a charged condensate.

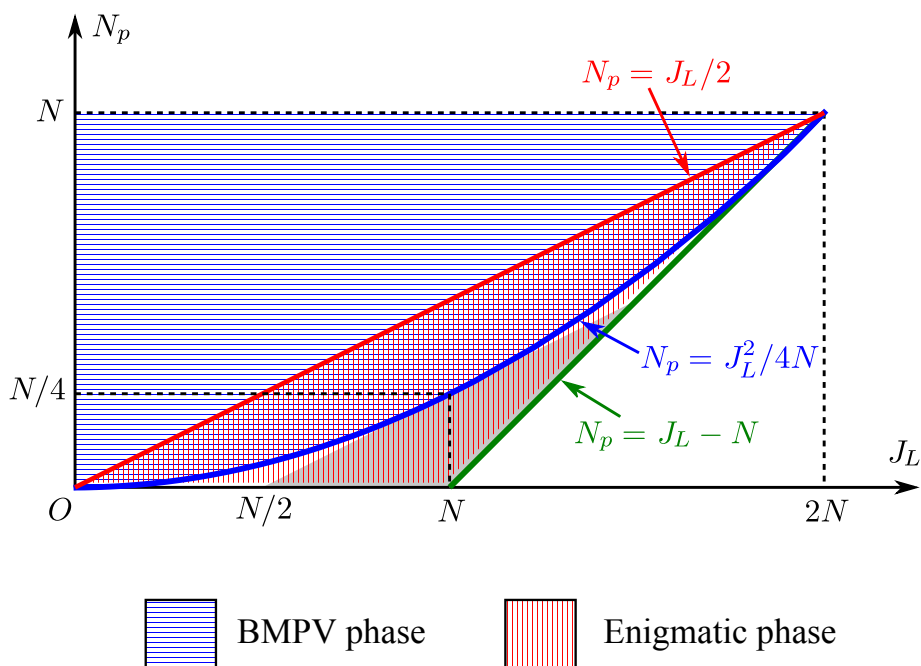


Figure 5. Phase diagram of D1-D5 CFT at the orbifold point.

The N_p - J_L diagram showing the BMPV and the enigmatic phases are plotted in figure 5. It is straightforward to see that

$$S_{\text{enigma}}^2 - S_{\text{BMPV}}^2 = \left(\frac{J_L}{2} - N_p \right)^2 \geq 0 \tag{2.14}$$

and thus the enigmatic phase is dominant over the BMPV phase and smoothly merges into it at the upper boundary of the “wedge” in figure 5. We emphasize that in the region where the enigmatic phase and the BMPV phase coexist the former dominates in entropy.

Spectral-flowed enigmatic phase. The enigmatic phase was constructed by splitting the CFT effective string into two parts. The long string carried all the excitations and thus the entropy and the short strings carried part of the angular momentum but no excitations. There is another configuration where the short strings carry part of the angular momentum but no entropy and that is gotten by making each short-string excitation of the form

$$\psi_{-1}^{+1} \psi_{-1}^{+2} \sigma_1^{++}. \tag{2.15}$$

In fact we can fill the fermions on the short strings up to a higher level η this way. For example, the short string for $\eta = 3$ corresponds to

$$\psi_{-3}^{+1} \psi_{-3}^{+2} \psi_{-2}^{+1} \psi_{-2}^{+2} \psi_{-1}^{+1} \psi_{-1}^{+2} \sigma_1^{++}. \tag{2.16}$$

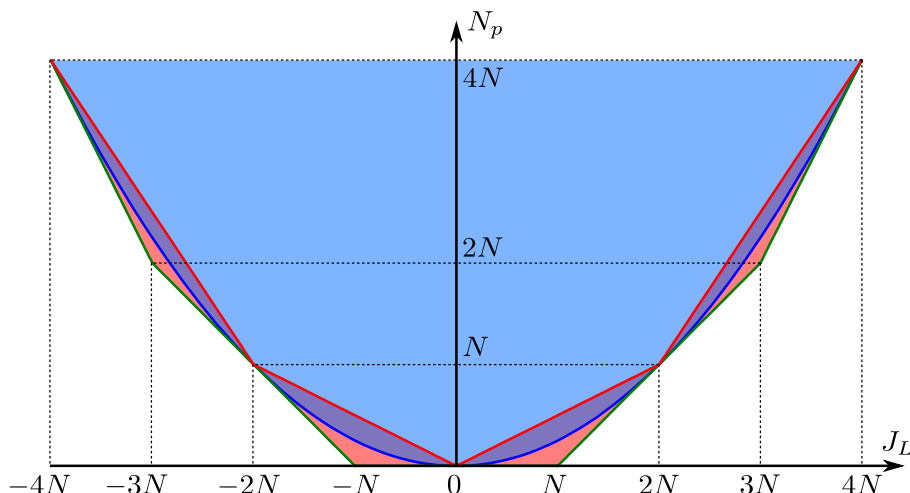


Figure 6. Spectral-flowed enigmatic phases

Such configurations are obtained from the original configuration by spectral flow (2.4) by 2η units. Using (2.3) to rewrite the enigmatic phase in terms of the dimension rather than the momentum:

$$S = 2\pi\sqrt{\left(L_0 - \frac{N}{4}\right)\left(L_0 - J_L + \frac{3N}{4}\right)} \quad (2.17)$$

one obtains the entropy of these spectral-flowed states:

$$S = 2\pi\sqrt{\left[L_0 - \eta J_L + \left(\eta^2 - \frac{1}{4}\right)N\right]\left[L_0 - (\eta + 1)J_L + \left((\eta + 1)^2 - \frac{1}{4}\right)N\right]}, \quad (2.18)$$

which is just a spectral-flowed version of the entropy formula by -2η units. This expression is valid in both NS and R sectors. We can then express this result in the Ramond sector in terms of the momentum using (2.3)

$$S = 2\pi\sqrt{[N_p - \eta J_L + \eta^2 N][N_p - (\eta + 1)J_L + (\eta + 1)^2 N]}. \quad (2.19)$$

As a simple example of this formula we see that we get the expression for the mirror image wedge ($J_L \rightarrow -J_L$) by taking $\eta = -1$. The region in which the spectral-flowed new phase exists is found by mapping the boundaries of the non-spectral-flowed new phase (2.12):

$$N_p - \eta J_L + \eta^2 N > 0, \quad N_p - (\eta + 1)J_L + (\eta + 1)^2 N > 0, \quad J_L(1 + 2\eta) - 2N_p - 2\eta(1 + \eta)N > 0. \quad (2.20)$$

In figure 6 we show four such enigmatic phases for $\eta = -2, -1, 0, 1$.

Note that, although the arguments above are for $M^4 = T^4$, the new phase should exist also for $M^4 = K3$ with the same entropy formula (2.11). This is because the structures we used above, such as effective strings and operators $\sigma^{\pm\pm}$, are common to both T^4 and $K3$.

2.3 Numerical evaluation of partition function

The analysis of the previous section showing a new “enigmatic” phase can be put on a firmer footing by looking at the partition function which counts all the states of the system

with given charges. We will evaluate the BPS partition function at the orbifold point of the CFT for both T^4 and $K3$ compactifications, and find that it indeed shows the growth expected from the entropy of the enigmatic phase. In the non-Cardy regime where the enigmatic phase exists, the BPS partition function is not easy to evaluate because we cannot use its modular properties. We overcome this problem by evaluating it numerically.

The BPS partition function computes the absolute degeneracy but is not protected under marginal deformations unlike the elliptic genus. We will also look at the (modified) elliptic genus on $K3$ (T^4) in the non-Cardy regime where the enigmatic phase exists to see if we find any trace of the enigmatic phase. The result is that these elliptic genera do not capture the enigmatic phase. This is as it should be, because the new phase exists in a region where the supergravity elliptic genus was found to match that of the CFT [16, 17]. Thus finding a new black object phase in the elliptic genera would have been a contradiction. In appendix D, we give an argument why the particular states of the form of a long string with excitations on it plus multiple short strings of length one do not contribute to the elliptic genus.

The readers who are not interested in the details of the computation can directly jump to section 2.3.3 where the final results are presented.

We begin by first defining the quantities we compute. The BPS partition function is defined as

$$\chi_{PF} = \text{Tr}_{RR;any,ground}[q^{L_0 - \frac{c}{24}} y^{J_L}], \quad q = e^{2\pi i \sigma}, \quad y = e^{2\pi i v} \quad (2.21)$$

where the trace is taken over all states in the left-moving Ramond sector and ground states in the right-moving Ramond sector. Namely, χ_{PF} counts BPS states only. The elliptic genus is defined as

$$\chi_{EG} = \text{Tr}_{RR}[(-1)^{J_L - J_R} q^{L_0 - \frac{c}{24}} y^{J_L}] \quad (2.22)$$

and the modified elliptic genus as

$$\chi_{MEG} = \text{Tr}_{RR}[(-1)^{J_L - J_R} (J_R)^2 q^{L_0 - \frac{c}{24}} y^{J_L}]. \quad (2.23)$$

where the traces are taken over all states in the left and right Ramond sectors. Even though the trace is taken over all states, it is easy to see that the elliptic genera only count states in the right-moving sector.

2.3.1 BPS partition function and elliptic genera on single copy of $K3$ and T^4

Let us first discuss the BPS partition function and elliptic genera on a single copy of T^4 and $K3$. Based on this, we will compute the BPS partition function and elliptic genera for symmetric products $\text{Sym}^N(K3)$ and $\text{Sym}^N(T^4)$.

- *Elliptic genus on $K3$*

The elliptic genus on $K3$ was found in [41, 42] and is given by

$$\chi_{EG}(q, y; K3) = 8 \left[\left(\frac{\vartheta_2(v, \sigma)}{\vartheta_2(0, \sigma)} \right)^2 + \left(\frac{\vartheta_3(v, \sigma)}{\vartheta_3(0, \sigma)} \right)^2 + \left(\frac{\vartheta_4(v, \sigma)}{\vartheta_4(0, \sigma)} \right)^2 \right]. \quad (2.24)$$

The elliptic genus is protected and is the same everywhere in the moduli space of $K3$ surfaces. From the definition of elliptic genus we see that the coefficient of $q^m y^l$ counts the difference between the number of bosonic and fermionic states with $L_0 = m + \frac{c}{24}$ and $J_L = l$. Thus we have

$$\chi_{EG}(q, y; K3) = \sum_{m \geq 0, l} \left(c_{K3}^B(m, l) - c_{K3}^F(m, l) \right) q^m y^l. \quad (2.25)$$

- *BPS partition function on $K3$*

The BPS partition function is not invariant under changes in moduli and thus depends on the point in the $K3$ moduli space where it is evaluated. So, in principle we should evaluate it at all points in the moduli space in order to show that it points toward the existence of the enigmatic phase. However, the BPS partition function can be computed only at special points in the $K3$ moduli space, and that is what we will content ourselves with.

The partition function for $K3$ can be computed [41] at the orbifold points¹⁰ in the $K3$ moduli space, where $K3$ can be written as T^4/\mathbb{Z}_l ($l = 2, 3, 4, 6$), and the BPS partition function can be extracted from it. For illustrative purposes, we present the BPS partition function at the orbifold point where $K3 = T^4/\mathbb{Z}_2$. This can be evaluated in a straightforward way using the results of [41] and is found to be¹¹

$$\chi_{PF}(q, y; K3 = T^4/\mathbb{Z}_2) = 2 \frac{\vartheta_2(v, \sigma)^2}{\eta(\sigma)^6} + 16 \left(\frac{\vartheta_4(v, \sigma)}{\vartheta_3(0, \sigma)} \right)^2 + 8 \left(\frac{\vartheta_2(0, \sigma)}{\vartheta_4(0, \sigma)} \right)^2 \left(\frac{\vartheta_2(v, \sigma)}{\vartheta_3(0, \sigma)} \right)^2. \quad (2.26)$$

From the definition of the partition function we can see that the coefficient of $q^m y^l$ counts the total number of states, both bosonic and fermionic, with $L_0 = m + \frac{c}{24}$ and $J_L = l$. Thus we have

$$\chi_{PF}(q, y; K3 = T^4/\mathbb{Z}_2) = \sum_{m \geq 0, l} \left(c_{K3}^B(m, l) + c_{K3}^F(m, l) \right) q^m y^l. \quad (2.27)$$

- *The modified elliptic genus on T^4*

The usual elliptic genus on T^4 vanishes identically because of extra fermion zero modes. On the other hand, the modified elliptic genus, which soaks up the extra fermion zero modes, is nonvanishing and given by [17]

$$\chi_{MEG}(q, y; T^4) = -2 \left[\frac{\theta_1(v, \sigma)}{\eta(\sigma)^3} \right]^2. \quad (2.28)$$

The coefficient of $q^m y^l$ again counts the difference between number of bosons and fermions of with $L_0 = m + \frac{c}{24}$ and $J_L = l$. However because half the fermion zero

¹⁰These orbifold points in the moduli space of $K3$ surfaces are not to be confused with the orbifold points in the moduli space of D1-D5 CFT where the target space is a symmetric orbifold of the $K3$ surface.

¹¹We ignored zero modes because they do not contribute to the BPS partition function for generic moduli of the parent T^4 .

modes are soaked up, the coefficient only counts the states built on the other half of the fermion zero modes [17]. To find the modified elliptic genus for the symmetric product, we will only need the total coefficient

$$\chi_{MEG}(q, y; T^4) = \sum_{m \geq 0, l} c_{MEG; T^4}(m, l) q^m y^l. \quad (2.29)$$

- *BPS partition function on T^4*

The BPS partition function for T^4 is straightforward to evaluate because it is a free theory. The result is found to be¹²

$$\chi_{PF}(q, y; T^4) = 4 \left[\frac{\vartheta_2(q, y)}{\eta(q)^3} \right]^2. \quad (2.30)$$

The coefficient of $q^m y^l$ counts the total number of states, both bosonic and fermionic, with $L_0 = m + \frac{c}{24}$ and $J_L = l$. However from the vanishing of the elliptic genus for T^4 we know that the number of bosonic and fermionic states are equal and so we have

$$\chi_{PF}(q, y; T^4) = \sum_{m \geq 0, l} c_{PF; T^4}(m, l) q^m y^l, \quad (2.31)$$

where

$$c_{T^4}^B(m, l) = c_{T^4}^F(m, l) = \frac{1}{2} c_{PF; T^4}(m, l). \quad (2.32)$$

2.3.2 BPS partition function and elliptic genera on $\text{Sym}^N(K3)$ and $\text{Sym}^N(T^4)$

Next we discuss the elliptic genus and BPS partition function on $\text{Sym}^N(K3)$ and the modified elliptic genus and BPS partition function on $\text{Sym}^N(T^4)$.

- *Elliptic genus on $\text{Sym}^N(K3)$*

In [43] the generating function for the elliptic genus on the symmetric product $\text{Sym}^N(K3)$ was found to be

$$\sum_{N \geq 0} p^N \chi_{EG}(q, y; \text{Sym}^N(K3)) = \prod_{n \geq 1, m \geq 0, l} \frac{1}{(1 - p^n q^m y^l)^{c_{K3}^B(mn, l) - c_{K3}^F(mn, l)}}. \quad (2.33)$$

We can expand the elliptic genus for $\text{Sym}^N(K3)$ as

$$\chi_{EG}(q, y; \text{Sym}^N(K3)) = \sum_{M \geq 1, L} C_{EG; K3}(N, M, L) q^M y^L, \quad (2.34)$$

where $C_{EG; K3}(N, M, L)$ counts the difference in bosonic and fermionic states with $L_0 = M + \frac{c}{24}$ and $J_L = L$ on $\text{Sym}^N(K3)$. Let us define

$$S_{EG; K3}(N, M, L) = \log |C_{EG; K3}(N, M, L)|. \quad (2.35)$$

By a slight abuse of terminology, we will refer to the logarithm of (modified) elliptic genus, such as $S_{EG; K3}(N, M, L)$ above, as “entropy”.

¹²Again, we ignored zero modes because they do not contribute for the generic moduli of T^4 .

- *BPS partition function on $\text{Sym}^N(K3 = T^4/\mathbb{Z}_2)$*

The generating function for the BPS partition function on the symmetric product $\text{Sym}^N(K3 = T^4/\mathbb{Z}_2)$ can be easily found using the techniques of [43] to be

$$\sum_{N \geq 0} p^N \chi_{PF}(q, y; \text{Sym}^N(K3 = T^4/\mathbb{Z}_2)) = \prod_{n \geq 1, m \geq 0, l} \frac{(1 + p^n q^m y^l)^{c_{K3}^F(mn, l)}}{(1 - p^n q^m y^l)^{c_{K3}^B(mn, l)}}. \quad (2.36)$$

We can expand the BPS partition function for $\text{Sym}^N(K3 = T^4/\mathbb{Z}_2)$ as

$$\chi_{PF}(q, y; \text{Sym}^N(K3 = T^4/\mathbb{Z}_2)) = \sum_{M \geq 1, L} C_{PF;K3}(N, M, L) q^M y^L, \quad (2.37)$$

where $C_{PF;K3}(N, M, L)$ counts the total number of states, both bosonic and fermionic, with $L_0 = M + \frac{c}{24}$ and $J_L = L$ on $\text{Sym}^N(K3 = T^4/\mathbb{Z}_2)$. We denote the associated entropy by

$$S_{PF;K3}(N, M, L) = \log C_{PF;K3}(N, M, L). \quad (2.38)$$

- *Modified elliptic genus on $\text{Sym}^N(T^4)$*

In [17] the generating function for the modified elliptic genus on $\text{Sym}^N(T^4)$ was found to be

$$\sum_{N \geq 0} p^N \chi_{MEG}(q, y; \text{Sym}^N(T^4)) = \sum s (p^n q^m y^l)^s c_{MEG}(mn, l). \quad (2.39)$$

The modified elliptic genus for $\text{Sym}^N(T^4)$ can be expanded as

$$\chi_{MEG}(q, y; \text{Sym}^N(T^4)) = \sum_{M \geq 1, L} C_{MEG;T^4}(N, M, L) q^M y^L, \quad (2.40)$$

where $C_{MEG;T^4}(N, M, L)$ counts the difference in bosonic and fermionic states with $L_0 = M + \frac{c}{24}$ and $J_L = L$ on $\text{Sym}^N(T^4)$. However because it soaks up half the zero modes it counts only the states built on the other half of the zero modes. We denote the associated “entropy” by

$$S_{MEG;T^4}(N, M, L) = \log |C_{MEG;T^4}(N, M, L)|. \quad (2.41)$$

- *BPS partition function on $\text{Sym}^N(T^4)$*

The generating function for the BPS partition function on the symmetric product $\text{Sym}^N(T^4)$ can also be easily found using the techniques of [43] to be

$$\sum_{N \geq 0} p^N \chi_{PF}(q, y; \text{Sym}^N(T^4)) = \prod_{n \geq 1, m \geq 0, l} \left(\frac{1 + p^n q^m y^l}{1 - p^n q^m y^l} \right)^{\frac{1}{2} c_{PF;T^4}(mn, l)} \quad (2.42)$$

where we used the relation (2.32). We can expand the partition function for $\text{Sym}^N(T^4)$ as

$$\chi_{PF}(q, y; \text{Sym}^N(T^4)) = \sum_{M \geq 1, L} C_{PF;T^4}(N, M, L) q^M y^L, \quad (2.43)$$

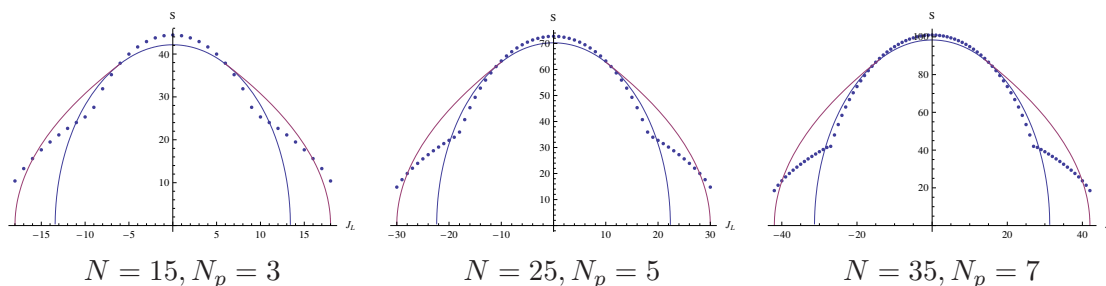


Figure 7. The logarithm of the elliptic genus for $\text{Sym}^N(K3)$.

where $C_{PF;K3}(N, M, L)$ counts the total number of states, both bosonic and fermionic, with $L_0 = M + \frac{c}{24}$ and $J_L = L$ on $\text{Sym}^N(T^4)$. We denote the associated entropy by

$$S_{PF;T^4}(N, M, L) = \log C_{PF;T^4}(N, M, L). \tag{2.44}$$

2.3.3 Numerical evaluation of partition functions and elliptic genera

Here we give the results of the numerical evaluation of the various entropies (2.35), (2.38), (2.41) and (2.44). We present the results by plotting $S(N, N_p, J_L)$ (blue dots) against J_L for different values of N with $\frac{N}{N_p} = 5$ along with the BMPV entropy (thin interior blue line) given by the Cardy formula (2.5) and the enigmatic phase entropy (2.11) (thin exterior red line).

- *Elliptic genus on $\text{Sym}^N(K3)$*

In figure 7 we plot $S_{EG;K3}(N, N_p, J_L)$ against J_L . We see that for small values of J_L the elliptic genus matches the Cardy formula but not the new phase. At some value of J_L “shoulders” appear in the elliptic genus and it deviates from the Cardy formula but still does not match the enigmatic phase entropy. Further plots for larger values of N, N_p keeping $N_p/N = 1/5$ fixed show us that the shoulders appear at larger values of J_L and are smaller. In fact, a numerical analysis hints at the bump coming from logarithmic corrections to the Cardy formula that vanish as $N, N_p \rightarrow \infty$. We thus conclude that the elliptic genus does not capture the enigmatic phase and asymptotes to the BMPV entropy.¹³

- *BPS partition function on $\text{Sym}^N(K3 = T^4/\mathbb{Z}_2)$*

In figure 8 we plot $S_{PF;K3}(N, N_p, J_L)$ against J_L . We see that the partition function for $\text{Sym}^N(K3)$ indeed captures the new phase. With larger values of N the match of the partition function to the enigmatic phase entropy (2.5) calculated in the large N limit in the previous subsection seems to get better but we were limited in our analysis by computational power. Although here we presented the result for $\text{Sym}^N(K3 = T^4/\mathbb{Z}_l)$ with $l = 2$, we worked out the other cases $l = 3, 4, 6$ as well and obtained similar behavior.

¹³This is consistent with [44] where it was shown that the $K3$ elliptic genus goes as (1.2) as long as all charges N, N_p, J_L are large, both in the Cardy and non-Cardy regimes.

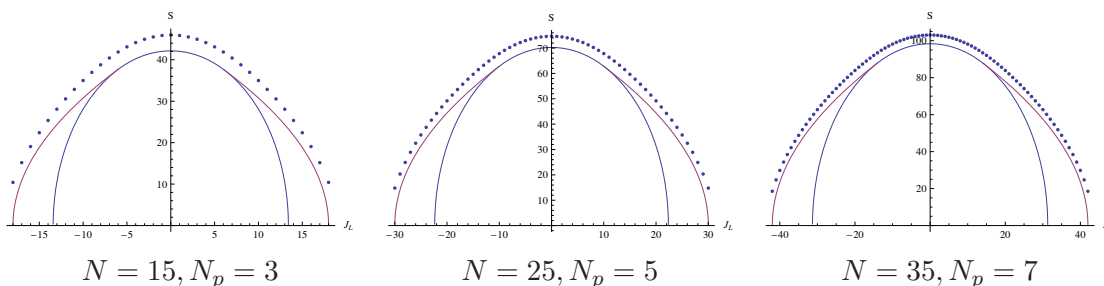


Figure 8. The logarithm of the BPS partition function for $\text{Sym}^N(K3 = T^4/\mathbb{Z}_2)$.

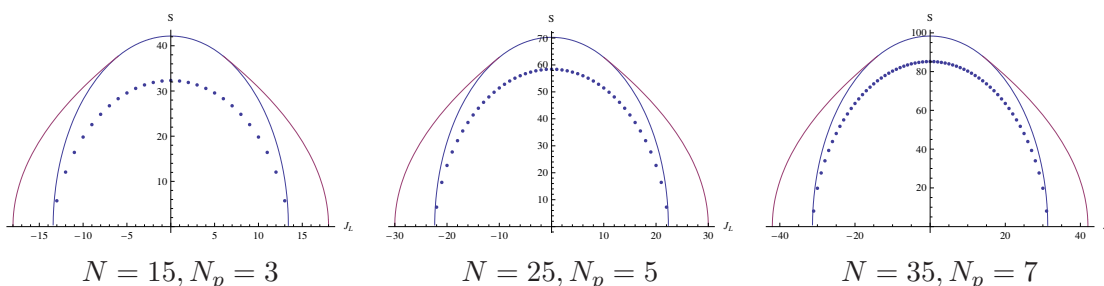


Figure 9. The logarithm of the modified elliptic genus for $\text{Sym}^N(T^4)$.

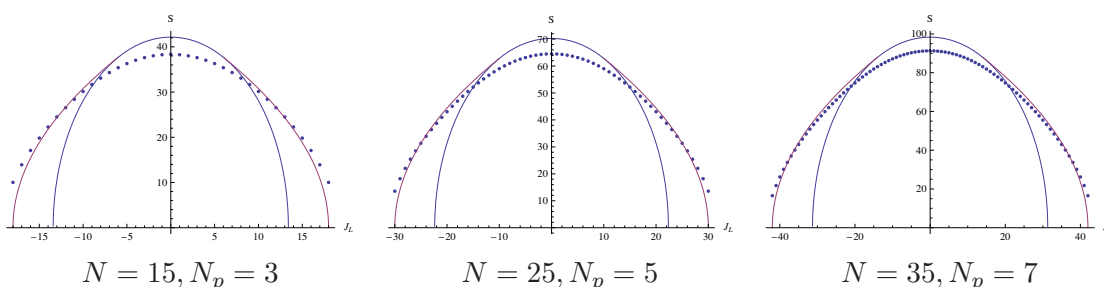


Figure 10. The logarithm of the BPS partition function for $\text{Sym}^N(T^4)$.

- *Modified elliptic genus on $\text{Sym}^N(T^4)$*
 In figure 9 we plot $S_{MEG;T^4}(N, M, L)$ against J_L . Just as the elliptic genus for $\text{Sym}^N(K3)$, the modified elliptic genus approaches the BMPV entropy for large N but fails to capture the enigmatic phase.
- *BPS partition function on $\text{Sym}^N(T^4)$*
 In figure 10 we plot $S_{PF;T^4}(N, N_p, J_L)$ against J_L . We see that the BPS partition function for $\text{Sym}^N(T^4)$ captures the enigmatic phase, just as that for $\text{Sym}^N(K3)$.

In conclusion, the numerical analysis of the BPS partition function, which counts the absolute degeneracy, confirms the existence of the new enigmatic phase with entropy (2.11) at the orbifold point of the D1-D5 CFT, both for T^4 and $K3$. On the other hand, the

(modified) elliptic genus, which is an index, does not capture the new enigmatic phase. One might naively take this as indicating that, once we depart the orbifold point of the CFT, the enigmatic phase gets lifted and is nowhere to be found in the supergravity regime. However, we will see that this is *not* so.

3 Supergravity analysis

Having established the existence of a new ensemble in the CFT let us now consider the possible bulk dual. From the structure of the boundary theory we might imagine that the dual configuration is a BMPV black hole surrounded by a maximally spinning super-tube [45] (which can be thought as sourcing the geometries dual to the maximally-spinning state) carrying *some* of its J_L . To systematically analyze possible bulk configurations we will first dualize to a IIA or M-theory frame where the full set of $U(1) \times U(1)$ symmetric configurations were classified in [26, 27, 46]. We will then argue that the putative duals are necessarily two-centered, and then use the bulk version of spectral flow symmetry to scan through all possible two center duals. More specifically, we “flow” any given two-centered configuration to a particular, tractable class of configurations where we can search for entropy-maximizing configurations.

3.1 Multi-centered Solutions in IIA/M-theory

Let us consider M-theory compactified on a T^6 (spanning $x_5, \dots, x_{10} = z$) to five dimensions.¹⁴ In [21, 47] the most general class of solutions preserving the same supersymmetries as three stacks of M2 branes were written down, and in [23] the most general class of solutions preserving a $U(1)$ isometry were classified (see also [26, 27, 46, 48]).

We will review the form of these solutions, using notation mostly¹⁵ following [49]. Our treatment will be somewhat concise; the reader is referred to [26, 49] for more details. The metric of the solutions is

$$ds_{11}^2 = -Z^{-2/3}(dt + k)^2 + Z^{1/3}ds_{\text{HK}}^2 + Z^{1/3} (Z_1^{-1}dx_{56}^2 + Z_2^{-1}dx_{78}^2 + Z_3^{-1}dx_{9z}^2), \quad (3.1)$$

with $Z = Z_1 Z_2 Z_3$. We mention in passing that this solution also requires a five dimensional gauge field but this will not be relevant for our analysis. This is the most general metric preserving the same supersymmetries as the three-charge black hole [21].

The 4-d metric ds_{HK}^2 is hyperkähler and if we take it to be tri-holomorphic (possessing a translational $U(1)$ isometry) then the most general solution is a Gibbons-Hawking space [50]

$$ds_{\text{HK}}^2 = V^{-1}(d\psi + A)^2 + V (dy_1^2 + dy_2^2 + dy_3^2), \quad dA = *dV \quad (3.2)$$

with $\psi \cong \psi + 4\pi$ the periodic coordinate. Here, and in what follows, $*$ denotes the Hodge dual with respect to the flat \mathbb{R}^3 base space with coordinates $y_{1,2,3}$.

¹⁴We could equally well consider M-theory on $K3 \times T^2$ and the five dimensional part of the discussion would go through unaltered.

¹⁵Our notation will differ in that our harmonic \tilde{M} is twice the M appearing in [49], $M_{\text{there}} = \frac{\tilde{M}_{\text{here}}}{2}$. To make this distinction clear we use \tilde{M} for M with our normalization.

The parameters entering into the above metric are

$$\begin{aligned} Z_I &= L_I + \frac{C_{IJK}K^J K^K}{2V}, & k &= \mu(d\psi + A) + \omega \\ \mu &= \frac{\tilde{M}}{2} + \frac{K^I L_I}{2V} + \frac{C_{IJK}K^I K^J K^K}{6V^2} \end{aligned} \tag{3.3}$$

with $I = 1, 2, 3$ and $C_{IJK} = |\epsilon_{IJK}|$. The one-form ω satisfies

$$*d\omega = \frac{1}{2} \left(V d\tilde{M} - \tilde{M} dV + K^I dL_I - L_I dK^I \right). \tag{3.4}$$

The solution is entirely specified by eight harmonic functions in \mathbb{R}^3 : V , K^I , L_I and \tilde{M}

$$V = \sum_p \frac{n_p}{r_p} + n_0, \quad K^I = \sum_p \frac{k_p^I}{r_p} + k_0^I, \quad L_I = \sum_p \frac{l_p^I}{r_p} + l_0^I, \quad \tilde{M} = \sum_p \frac{m_p}{r_p} + m_0. \tag{3.5}$$

The labels $p = 1, \dots, N$ run over the number of centers with $r_p = |\vec{x} - \vec{x}_p|$ the distance from each center in the flat \mathbb{R}^3 metric. The choice of constants in the harmonic functions

$$h = \{n_0, k_0^I, l_0^I, m_0\} \tag{3.6}$$

fixes the asymptotic structure of the spacetime. The charges

$$\Gamma_p = \{n_p, k_p^I, l_p^I, m_p\} \tag{3.7}$$

at a given center p correspond, in the M-theory frame, to KK-monopole, M5, M2, and KK-momentum charge, respectively, where the monopole and momentum charge are along the ψ circle. As usual, when we reduce M-theory to IIA along ψ these respectively become D6, D4, D2, and D0 charges, and we will mostly use this language.¹⁶

The charges that appear in the harmonic functions above are dimensionful quantities that characterize a supergravity solution, and can be related to the quantized brane charges of the solution (that give the CFT charges) via proportionality constants that depend on the moduli and coupling constants of the solution. These relations depend on the duality frame, and can be straightforwardly derived or found in many references (see for example eq. (2.3) in [24] or appendix D of [49]). To un-clutter notation, in the rest of the paper we pick a particular set of values for the moduli such the supergravity charges are always equal to the quantized charges.

3.1.1 Entropy, Angular momentum and CTCs

The solutions given above generically carry angular momentum in \mathbb{R}^3 coming from crossed electric and magnetic fields (recall that in four dimensions D4 branes and D2 branes are electromagnetic duals of each other, and so are D6 branes and D0 branes). This can be read off from the asymptotic value of ω as (see e.g. [46])

$$\vec{J}^{(3)} = \sum_{p < q} \frac{\langle \Gamma_p, \Gamma_q \rangle}{r_{pq}} \vec{r}_{pq} \tag{3.8}$$

¹⁶In the conventions used in this paper the numbers appearing in (3.7) are the integer charges of KK-monopole, M5, M2 and KK-momentum. For details see appendix E.

where $\vec{r}_{pq} \equiv \vec{x}_p - \vec{x}_q$ and

$$\langle \Gamma_p, \Gamma_q \rangle = n_p m_q + k_p^I l_I^q - l_I^p k_q^I - m_p n_q \quad (3.9)$$

gives the electromagnetic pairing.

A given center Γ_p may correspond to a black object with a horizon at $r_p = 0$; the area can be computed by evaluating

$$S(r) = 2\pi\sqrt{D(r)} = 2\pi\sqrt{Z_1 Z_2 Z_3 V - \mu^2 V^2} \quad (3.10)$$

at the horizon giving (in terms of the charges) the $E_{7(7)}$ invariant

$$\begin{aligned} D(\Gamma_p) = & -\frac{1}{4}m_p^2 n_p^2 - \frac{1}{6}m_p C_{IJK} k_p^I k_p^J k_p^K - \frac{1}{2}m_p n_p k_p^I l_I^p - \frac{1}{4}(k_p^I l_I^p)^2 \\ & + \frac{1}{6}n_p C^{IJK} l_I^p l_J^p l_K^p + \frac{1}{4}C^{IJK} C_{IMN} l_J^p l_K^p k_p^M k_p^N. \end{aligned} \quad (3.11)$$

The function $D(r)$ is proportional to the $g_{\psi\psi}$ component of the metric, and so its positivity effects the causal structure of the spacetime; if $D(r) < 0$ in some region the metric will contain closed timelike curves (CTCs) and must be discarded as unphysical. This constraint will play an important role in what follows.

Another necessary but not sufficient set of conditions for the absence of CTCs are the $N - 1$ so-called integrability (or ‘‘bubble’’) equations

$$\sum_{q=1, q \neq p}^N \frac{\langle \Gamma_p, \Gamma_q \rangle}{r_{pq}} = \langle h, \Gamma_p \rangle \quad (3.12)$$

which, for two centers, fix the inter-center separation.

The condition (3.12) is a no-CTC condition in the neighborhood of the centers but a more general no-CTC condition is the global positivity of

$$Z_1 Z_2 Z_3 V - \mu^2 V^2 - |\omega|^2 \geq 0, \quad (3.13)$$

which ensures the existence of a time function [27]. This is, in general, a difficult condition to check but it will play a role in simplifying our analysis. We will often employ the weaker (necessary but not sufficient) condition $D(r) > 0$ to constrain our choice of solutions.

3.1.2 Gauge symmetries and ‘‘Spectral Flow’’

The solutions above are invariant [48] under a family of ‘‘gauge transformations’’¹⁷ parametrized by three constants, g^I :

$$\begin{aligned} V & \rightarrow V, & K^I & \rightarrow K^I + g^I V, \\ L_I & \rightarrow L_I - C_{IJK} g^J K^K - \frac{1}{2} C_{IJK} g^J g^K V, \\ \tilde{M} & \rightarrow \tilde{M} - g^I L_I + \frac{1}{2} C_{IJK} g^I g^J K^K + \frac{1}{6} C_{IJK} g^I g^J g^K V. \end{aligned} \quad (3.14)$$

¹⁷These are generated by gauge transformations of the 10-dimensional B-field in the IIA frame.

Another set of transformations¹⁸ parametrized by γ_I , are [51]

$$\begin{aligned}
 \tilde{M} &\rightarrow \tilde{M}, & L_I &\rightarrow L_I - \gamma_I \tilde{M}, \\
 K^I &\rightarrow K^I - C^{IJK} \gamma_J L_K + \frac{1}{2} C^{IJK} \gamma_J \gamma_K \tilde{M}, \\
 V &\rightarrow V + \gamma_I K^I - \frac{1}{2} C^{IJK} \gamma_I \gamma_J L_K + \frac{1}{6} C^{IJK} \gamma_I \gamma_J \gamma_K \tilde{M}.
 \end{aligned} \tag{3.15}$$

While the latter are *not* symmetries of the solutions they are clearly related to the transformation of (3.14) via electric-magnetic duality. These transformations can, in fact, be generated by U -dualities and, in the IIB frame, by diffeomorphisms (see [51] for more details). As the entropy function (3.11) is, by construction, U -duality invariant these transformations preserve the entropy of the centers. The charges at each center, however, are not invariant so we can use these transformations to transform the charges to a convenient form. Thus these symmetries will greatly simplify the task of scanning through putative bulk dual solutions. We will generally refer to these as g - and γ -transformations, respectively.

3.1.3 T-dualizing to the IIB frame

The metrics given above correspond to solutions of IIA string theory compactified on T^6 with D6, D4, D2, D0 charges but, as we are interested in the D1-D5 system in IIB, we must dualize to this frame. An appropriate set of dualities consists of a KK reduction to IIA on x_9 (rather than ψ), followed by three T -dualities along x_5 , x_6 and $z = x_{10}$ yielding the following charges.

$$\left\{ \begin{array}{l} M2(56) \\ M2(78) \\ M2(9z) \end{array} \right\} \xrightarrow{\text{KK on } x_9 \text{ to IIA}} \left\{ \begin{array}{l} D2(56) \\ D2(78) \\ F1(z) \end{array} \right\} \xrightarrow{T_{56z}} \left\{ \begin{array}{l} D1(z) \\ D5(5678z) \\ P(z) \end{array} \right\} \tag{3.16}$$

while the M5 charges become dipole charges in IIB

$$\left\{ \begin{array}{l} m5(\psi 789z) \\ m5(\psi 569z) \\ m5(\psi 5678) \end{array} \right\} \xrightarrow{\text{KK on } x_9 \text{ to IIA}} \left\{ \begin{array}{l} d4(\psi 78z) \\ d4(\psi 56z) \\ ns5(\psi 5678) \end{array} \right\} \xrightarrow{T_{56z}} \left\{ \begin{array}{l} d5(\psi 5678) \\ d1(\psi) \\ kk(\psi 5678; z) \end{array} \right\} \tag{3.17}$$

The final solution has a KK-monopole dipole charge along the $\psi 5678$ directions with its special transverse circle in the z direction, denoted by $kk(\psi 5678; z)$. The original M-theory KK and momentum modes along the Gibbons-Hawking isometry direction ψ (corresponding upon ψ -reduction to D6 and D0 in the IIA) are relatively inert under these transformations and go over to $kk(56789z; \psi)$ and $P(\psi)$ in IIB.

The resultant NSNS fields are [49]

$$ds_{\text{IIB}}^2 = -\frac{1}{Z_3 \sqrt{Z_1 Z_2}} (dt + k)^2 + \sqrt{Z_1 Z_2} ds_{\text{HK}}^2 + \frac{Z_3}{\sqrt{Z_1 Z_2}} (dz + A^3)^2 + \sqrt{\frac{Z_1}{Z_2}} dx_{5678}^2 \tag{3.18}$$

¹⁸These transformations were called ‘‘Spectral Flow’’ transformations in [51] because when the solutions are dualized to asymptotically $AdS_3 \times S^3$ IIB solutions (as explained below) one of them corresponds to a spectral flow of the dual CFT.

$$e^\Phi = \frac{Z_1}{Z_5}, \quad B_{\mu\nu} = 0 \tag{3.19}$$

and there is also an RR potential, $C^{(2)}$, corresponding to the D1 and D5 charge. In order to determine when this metric is asymptotically-AdS (as we will explain in detail in appendix A) we will need

$$A^3 = \frac{K^3}{V}(d\psi + A) + \xi^3 - \frac{1}{Z_3}(dt + k), \quad *d\xi^3 = -dK^3. \tag{3.20}$$

When there are no dipole charges, ($K^I = 0$), we see from (3.3) that the Z_I reduce to simple harmonic functions and the metric above is the usual D1-D5-P black hole metric.

3.1.4 AdS₃×S³ and the AdS/CFT Dictionary

If we consider a system with $n \neq 0$ (net D6 charge in IIA) then we can take a decoupling limit such that the solution is asymptotically AdS₃×S³/Z_{*n*}. We review the AdS/CFT dictionary for these solutions as we will need it in what follows; for details of the decoupling limit the reader is referred to appendix A.¹⁹

We consider a total charge

$$\Gamma = \{n, k^I, l_I, m\} \tag{3.21}$$

and we set all the constants $h = \{n_0, k_0^I, l_I^0, m_0\}$ to zero except $l_3^0 = 1$ and

$$m_0 = -\frac{k^3}{n}. \tag{3.22}$$

The choice to set $l_3^0 \neq 0$ yields AdS asymptotics and the requirement²⁰ that $\langle \Gamma, h \rangle = 0$ then fixes the choice of m_0 . Of course if $k^3 = 0$ then even $m_0 = 0$ (but we do not allow $n = 0$ as this does not generate an AdS₃×S³ geometry). Note that as a consequence of these asymptotics the integrability equations (3.12) imply that centers that do not have either D6 charge or the D4 charge k_p^3 cannot form bound states inside AdS₃ (otherwise the right hand side of (3.12) is zero).

Most CFT quantum numbers can be read off from the asymptotic values of the charges as follows

$$\begin{aligned} N_1 \sim Z_1^{(1)} \sim l_1 + \frac{k^2 k^3}{n}, & \quad N_p \sim Z_3^{(1)} \sim l_3 + \frac{k^1 k^2}{n}, \\ N_5 \sim Z_2^{(1)} \sim l_2 + \frac{k^1 k^3}{n}, & \quad \mathcal{J}_L \sim 2\mu^{(1)} \sim m + \frac{k^I l_I}{n} + \frac{2k^1 k^2 k^3}{n^2} \end{aligned} \tag{3.23}$$

where the superscript “(1)” on a quantity f means to pick out the coefficient of the order $1/r$ term from the large r expansion of f . For Z_1, Z_2 this is the leading term but for Z_3 the leading piece is the constant l_3^0 . Note that the constraint (3.22) guarantees that μ has no leading constant piece.

¹⁹See also the appendix of [51].

²⁰Which simply follows from also summing over the index p on both sides of eq. (3.12) and using the anti-symmetry of the pairing $\langle \cdot, \cdot \rangle$.

As we explained above, the quantized charges that characterize the CFT are related to the “supergravity” charges that one obtains from the asymptotics of the warp factors via proportionality constants that depend on the moduli and coupling constants of the solution. However, given that our phase is a hybrid between the BMPV phase and the maximally spinning phase, we can always use the known relation between these CFT phases and their dual bulk solutions to relate the supergravity and CFT charges. Alternatively, we can work at some values of the moduli where the supergravity and quantized charges are always equal, which is what we will do through the rest of this paper.

In particular, the charge \mathcal{J}_L is to be identified with J_L of the CFT up to a sign that we will discuss below. Furthermore, as with J_L , we will define a bulk charge \mathcal{J}_R related to the CFT charge J_R up to a sign. The charge \mathcal{J}_R comes from the $\text{SO}(3) \cong \text{SU}(2)$ angular momentum, $\vec{J}^{(3)}$, of the \mathbb{R}^3 base of the solutions (which becomes one of the $\text{SU}(2)$'s in the $\text{SO}(4)$ isometry group of S^3 in the near horizon geometry) so can be read off from the asymptotic value of ω

$$\mathcal{J}_R \sim 2\omega^{(1)}. \tag{3.24}$$

Unlike the other CFT charges \mathcal{J}_R depends not on the total bulk charge but on the distribution of charges between the centers. For two centers (to which we will turn presently) this reduces to

$$\mathcal{J}_R = \langle \Gamma_1, \Gamma_2 \rangle. \tag{3.25}$$

Note that we could just as well have chosen $\mathcal{J}_R = \langle \Gamma_2, \Gamma_1 \rangle$ which would differ from the definition above by a minus sign. To fix conventions however we will *define* \mathcal{J}_R as above and then relate it to the J_R in the CFT (which we have defined to be positive) via $J_R = \pm \mathcal{J}_R$.

3.1.5 A Note on Signs

When identifying the CFT quantum numbers with those of the bulk we must be careful to incorporate potential physically-meaningful sign differences. The sign of $N_1 N_5$ is fixed by the requirement of giving a positive AdS_3 central charge and the sign of N_p is fixed with respect to this.²¹

The angular momenta \mathcal{J}_L and \mathcal{J}_R are related to those in the CFT but there is no canonical way to fix the signs. In the CFT we have taken, without loss of generality, $J_L, J_R > 0$ and we would like to do the same in the bulk. From the expression for \mathcal{J}_L we see that we can flip its sign simply by sending k^I, m to $-k^I, -m$ which is a symmetry of the solution. This also flips the sign of \mathcal{J}_R as the intersection product $\langle \Gamma_1, \Gamma_2 \rangle$ is odd under this symmetry. As mentioned above we also have the further freedom to change the sign of \mathcal{J}_R by switching the order $\Gamma_1 \leftrightarrow \Gamma_2$ but for notational clarity let us fix the definition of the scalar quantity $\mathcal{J}_R := \langle \Gamma_1, \Gamma_2 \rangle$ and then define $\vec{J}_R = \mathcal{J}_R \hat{x}_{12}$ with \hat{x}_{12} a unit vector between the two centers. In order to match conventions with the CFT we will measure the angular momentum at infinity along an axis aligned with \vec{J}_R so that $J_R > 0$. In terms of \mathcal{J}_R this gives $J_R = \pm \mathcal{J}_R$. Thus we can always arrange for $J_L, J_R > 0$ in the bulk but, as we will

²¹When $M^4 = T^4$, neither sign of N_p will break supersymmetry. However, in the $\mathcal{N} = 2$ formalism we are working in, only one sign is manifestly supersymmetric and allowed.

see below, once we have fixed charge conventions such that $J_L > 0$, we have to check the sign of \mathcal{J}_R to determine if $J_R = \mathcal{J}_R$ or $-\mathcal{J}_R$.

3.2 Two-centered Solutions in $\text{AdS}_3 \times \text{S}^3$

While a general bulk solution in the class considered above may have many centers we will now argue that the putative duals to the new CFT phase must be two-center configurations. This follows from the observation that an N -center solution has $3N - 3$ parameters ($3N$ given by \vec{r}_p minus the three center of mass parameters) constrained by $N - 1$ equations giving a $2N - 2$ dimensional solution space. Generically, each point in this space corresponds to a different value of \mathcal{J}_R via (3.8). As the leading entropy comes from summing the entropy of each center and does not depend on the locations of the centers, an N -center configuration generically has a fixed (leading) entropy but a range of \mathcal{J}_R .

The new phase in the CFT, however, is characterized by a fixed value of J_R that maximizes the entropy. We thus expect a bulk configuration with fixed \mathcal{J}_R . It is not hard to see that this corresponds to $N = 2$; for two centers $J^{(3)}$ is fixed and only its orientation is unfixed (yielding two parameters $\{\theta, \phi\}$). Thus we can restrict our analysis to two-center configurations.

3.2.1 Stability and Smoothness

To further constrain the problem, let us consider the partition of a fixed total charge into two centers $\Gamma = \Gamma_1 + \Gamma_2$ and the entropy of the associated configuration

$$S_{2\text{-center}} = S(\Gamma_1) + S(\Gamma_2). \tag{3.26}$$

One might naively imagine, based on the intuition that black holes are thermodynamic ensembles, that such a partition is always entropically disfavorable as combining two ensembles generally increases the total entropy:

$$S_{1\text{-center}}(\Gamma_1 + \Gamma_2) \stackrel{?}{>} S_{2\text{-center}} = S(\Gamma_1) + S(\Gamma_2). \tag{3.27}$$

It is clear, however, from examples such as the entropy enigma of [10] that such intuition is misguided and there are examples when a two-center configuration has larger entropy than a single-center configuration. Because of this, and because of the non-vanishing constant value of \mathcal{J}_R observed in the CFT, we restrict ourselves to two-center configurations and look for the ones with the most entropy.

To find them, one would need to do a stability analysis based on maximizing the total entropy of a partition into two charges:

$$S_{2\text{-center}} = S(\Gamma - \Gamma_2) + S(\Gamma_2), \tag{3.28}$$

If the configuration is stable (locally entropy-maximizing), the Hessian of $S_{2\text{-center}}$ with respect to Γ_2 should have only negative eigenvalues. If there are some positive eigenvalues, the configuration is entropically unstable against shedding charge from one center to the other.

Although the analysis of the Hessian for the general partition Γ_2 is technically rather difficult, there is one situation where one might expect stability: when one center is smooth and carries no macroscopic or microscopic entropy — such a center can no longer shed charge to the other center without producing closed timelike curves. Such smooth centers, first discussed in [26, 27], correspond in four dimensions to D6 branes with Abelian worldvolume fluxes [52], and have also appeared in the $\mathcal{N} = 2$ entropy enigma [11]. In appendix C we will demonstrate local entropic stability for two-center configurations where all the entropy is carried by one center.

While other two center configurations *might* be entropically stable, they are probably non-generic and thus will impose many additional charge constraints. Although we cannot entirely rule out stable configurations with two horizons, motivated by the entropy enigma of [11] and the fact that configurations with a smooth center live on the boundary of charge space and are isolated (in the sense of not being continuously connected to other charge configurations), we will restrict our analysis to configurations with one smooth center.

Requiring $S(\Gamma_2) = 0$ and smoothness²² at r_2 fixes the charge Γ_2 to satisfy [26, 27, 49]

$$l_I = -\frac{C_{IJK}k^Jk^K}{2n}, \quad m = \frac{k^1k^2k^3}{n^2} \tag{3.29}$$

from which it follows [52] that center “2” carries no microscopic entropy as it is gauge-equivalent (by choosing the appropriate g^I in eq. (3.14)) to n D6-branes in IIA or to a \mathbb{Z}_n quotient singularity in M-theory.

Thus we can reduce our problem to considering solutions specified by the following charges and asymptotics

$$\begin{aligned} \Gamma_1 &= \{1 - \alpha, \{k^1, k^2, k^3\}, \{l_1, l_2, l_3\}, m\}, \\ \Gamma_2 &= \{\alpha, \{\alpha p^1, \alpha p^2, \alpha p^3\}, \{-\alpha p^2 p^3, -\alpha p^1 p^3, -\alpha p^1 p^2\}, \alpha p^1 p^2 p^3\}, \\ h &= \{0, \{0, 0, 0\}, \{0, 0, 1\}, -k^3 - \alpha p^3\} \end{aligned} \tag{3.30}$$

where h denotes the “vector” of constants in the harmonic functions. One can check that Γ_2 satisfies (3.29) and so corresponds to a smooth center with $S(\Gamma_2) = 0$ for any choices of α, p_i . By charge quantization, all the entries of Γ_2 , such as $\alpha, \alpha p^1$, and $\alpha p^2 p^3$, are assumed to be integers. Note we have taken the total KKM/D6 charge to be 1. When this charge is n the decoupling limit discussed in appendix A gives an $\text{AdS}_3 \times \text{S}^3 / \mathbb{Z}_n$ space. Nevertheless, since the CFT phase we found exists in the standard unquotiented orbifold theory, we are only interested in asymptotically $\text{AdS}_3 \times \text{S}^3$ solutions so we restrict to $n = n_1 + n_2 = 1$.

The smoothness condition (3.29) insures that a certain center is smooth in all duality frame. Nevertheless, in the D1-D5-P duality frame in which we are working it is also possible to have smooth centers that correspond in the IIA frame not to fluxed D6 branes but to fluxed D4 branes that have a nonzero k^3 . These are the supertubes dual to the maximally spinning phase, and can be thought of as coming from (3.30) by taking the limit $\alpha \rightarrow 0$ keeping αp^3 fixed (note that this limit is rather formal, because we take α to

²²If there is a singularity at $r = r_2$ this is usually associated with a microscopic horizon and subleading entropy so we can re-apply the entropy maximization argument above including subleading corrections.

be an integer). When the smooth center is a supertube, the KKM charge of the first center is one.

3.2.2 Spectral Flow in the Bulk

While our analysis of the last subsection has reduced the problem to considering all two-center configurations with one smooth center, this is still a rather daunting problem. On the other hand these solutions enjoy a great deal of symmetry arising from (3.14)–(3.15) and we can use this to simplify our analysis.

From (3.15) we see that a general γ -flow modifies the asymptotics and may not preserve an asymptotically $AdS_3 \times S^3$ form of the metric. Recall that the latter requires that only m_0 and l_3^0 are non-vanishing and that they satisfy (3.22). Moreover, as mentioned above, we want to keep the total D6-charge equal to one.

Let us see how these constraints restrict the transformations we can perform. First since gauge transformations (g^I -flows) preserve the solution we are free to perform them with impunity. On the other hand, a general γ_I -flow modifies V in a way dependent on all the other harmonics, and hence will generically modify the asymptotics. Since we are interested in keeping the $AdS_3 \times S^3$ asymptotics, it is not hard to see from (3.30) that we can only use a γ -flow with a nonzero γ_3 . In the IIB duality frame we are in, this is a geometrized component of the U -duality group, and is the bulk dual to spectral flow in the CFT [51].

To ensure that γ_3 does not modify V , we first have to use our gauge-freedom to set K^3 to vanish asymptotically. This is simply accomplished by $g^3 = -k^3 - p^3\alpha$. We are then free to flow by γ_3 and find this affects the solution asymptotically as follows:

$$\tilde{Z}_1 \sim Z_1, \quad \tilde{Z}_2 \sim Z_2, \tag{3.31}$$

$$\tilde{Z}_3 \sim Z_3 - 2\gamma_3\mu + (\gamma_3)^2 Z_1 Z_2 \tag{3.32}$$

$$\tilde{\mu} \sim \mu - \gamma_3 Z_1 Z_2 \tag{3.33}$$

with \sim meaning that the leading asymptotic terms (as well as the subleading term in Z_3) Recalling (3.23) and comparing this with (2.4) we see the above maps to spectral flow in the CFT by $\eta = \mp\gamma_3$ for $\mathcal{J}_L = \pm J_L$. As we will fix conventions such that $\mathcal{J}_L = J_L$ this gives $\eta = -\gamma_3$.

3.2.3 Spectral Flowing to BMPV plus Supertube

We will now take advantage of the above transformations to flow arbitrary charges of the form (3.30) to a more tractable form. We first spectral flow using the following transformations

$$g^3 = -k^3 - p^3\alpha \quad \text{followed by} \quad \eta = -\gamma_3 = -\frac{1}{k^3 + p^3\alpha - p^3}. \tag{3.34}$$

This has the effect of removing the D6 charge from Γ_2 and turning the latter into a supertube. After this Γ_1 still generically has non-vanishing D4 charges but we can use a gauge transformation (which has no effect on the CFT quantum numbers) to set k'^I (these flowed charges are generally inequivalent to those of (3.30)) to zero via

$$(g^1, g^2, g^3) = (-k'^1, -k'^2, -k'^3). \tag{3.35}$$

The resultant charge vectors after these transformations are

$$\begin{aligned}
 \Gamma_{\text{bmpv}} &= \{1, \{0, 0, 0\}, \{Q_1, Q_2, Q_3\}, m\}, \\
 \Gamma_{\text{tube}} &= \left\{0, \{0, 0, d\}, \{q_1, q_2, 0\}, \frac{q_1 q_2}{d}\right\}, \\
 h &= \{0, \{0, 0, 0\}, \{0, 0, 1\}, -d\}.
 \end{aligned}
 \tag{3.36}$$

The relation between these charges and those of (3.30) can be found in appendix B. As indicated in the labeling in (3.36), the first center is nothing but a BMPV black hole while the second is a maximally spinning supertube. As we explain below we have chosen this choice of spectral flow to simplify our analysis.

One may wonder if a spectral flow by a fractional flow parameter (3.34) is allowed. Actually, the spectral flow is a transformation which maps a legitimate configuration into another legitimate configuration in both supergravity and the CFT, and is defined in principle for *any* flow parameter. Therefore, such flows are indeed allowed.

It is true that on the CFT side the flow parameter must be integer quantized if one wants to map a state in a sector to another state *in the same sector* with the same periodicity of fermions. Non-integral spectral flows, on the other hand, change the fermion periodicity both in the boundary and bulk. However, they also modify the VEV of the asymptotic gauge field in a compensating way so that the bulk geometry remains regular in a suitable sense; e.g., supersymmetry stays preserved due to the modified VEV of the gauge field (see [38] and references therein for more details). By assumption our solution (3.30) is dual to the original D1-D5 CFT which is in the Ramond sector. After flowing by η units the solution (3.36) will not be in the Ramond sector if η is non-integral but this is of no consequence as we ultimately flow this solution back by $-\eta$ units once we have found the maximal entropy configuration. Thus our final configuration will once more be in the Ramond sector (in fact we will see in our analysis that the entropy-maximizing value of η turns out to be integral so such concerns are moot).

The astute reader may also notice that the spectral flowed charges (3.36), whose explicit expressions can be found in appendix B, are not integers in general and wonder if they are allowed. However, note that we initially started with integral charges (3.30) and thus a manifestly regular geometry. Spectral flow merely gives different frames to look at the same physical situation, and hence a regular configuration is mapped into a regular configuration again, no matter how it may look. In the present case, the fractional charges are allowed because of the gauge field VEV mentioned above, which modifies the charge quantization. This point is perhaps easier to understand in the IIB frame (3.18), where the spectral flow transformation is nothing but a coordinate change of the ψ - z torus [51]. A fractional flow mixes ψ and z in a non-standard way such that they are not independently periodic. However, a coordinate transformation does not change the physical torus, which remains regular. The fractional charges just reflect the non-standard periodicity of the torus coordinates and pose no problem at all.

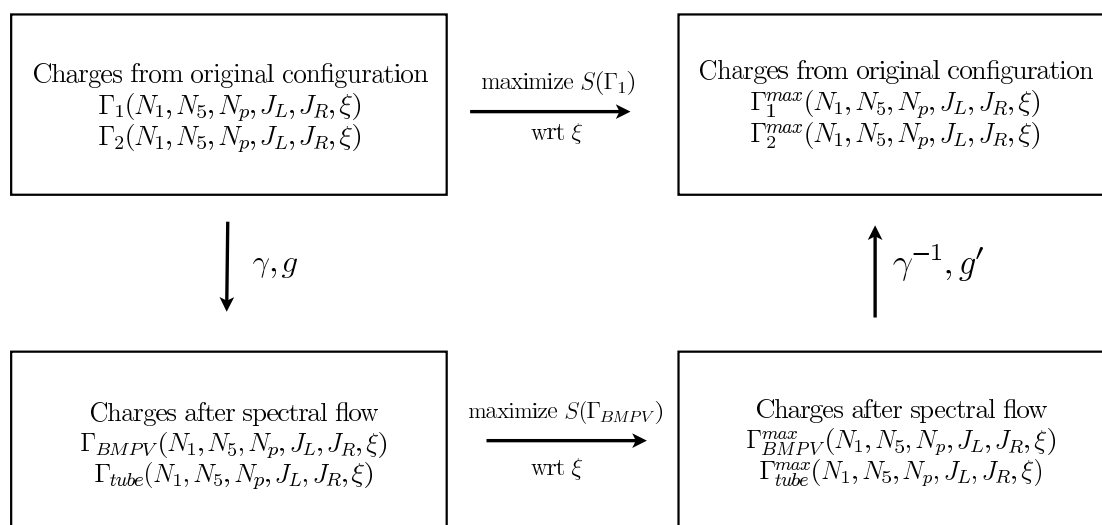


Figure 11. We want to maximize the bulk entropy with charges given in (3.30) with respect to parameters (collectively denoted by ξ) describing the distribution of charges between the centers; this procedure is described by the top horizontal arrow, and is quite non-trivial. Alternatively we can spectral flow and gauge transform to the BMPV plus tube configuration with charges given in (3.36) (left vertical arrow) and then maximize the entropy (lower horizontal arrow). We can then spectral flow the configuration back (right vertical arrow) to get the required maximum entropy solution dual to the CFT.

3.3 The BMPV plus Supertube System

Thus far we have argued that it is possible to use the bulk analog of spectral flow (combined with gauge transformations that do not affect the CFT) to transform a two-center solution where one center carries no entropy and the other has an arbitrary set of charges to a BMPV black hole surrounded by a supertube (3.36). The spectral flows and gauge transformations do not alter the entropy of the bulk configuration, and the particular γ_3 spectral flow also leaves the smooth center smooth (although it may change it from a D6 center to a supertube). On the other hand the charges (3.36) are rather simple and maximizing the entropy of the total system with fixed CFT charges is relatively straightforward. This process is described in figure 11.

The reason to take this somewhat indirect approach is that it is rather non-trivial to maximize $S(\Gamma_1)$ (with Γ_1 arbitrary) with respect to fixed CFT charges while making sure that the bulk solution stays regular and free of CTC's. On the other hand, it is very easy to understand the origin of CTC's in the BMPV+supertube system (they appear when the charge of the supertube and those of the BMPV black hole are opposite, or when either object has too much angular momentum) and hence it is much more straightforward to maximize $S(\Gamma_{\text{bmpv}})$ and to relate the CFT charges to the parameters appearing in (3.36).

In fact the relation is simply given by

$$\begin{aligned}
 N_1 &= Q_1 + q_1, & N_5 &= Q_2 + q_2, & N'_p &= Q_3 \\
 \mathcal{J}'_L &= d N'_p + \frac{q_1 q_2}{d} + m, & \mathcal{J}_R &= \frac{q_1 q_2}{d} - d N'_p \\
 r_{12} &= \frac{q_1 q_2}{d^2} - N'_p = \frac{\mathcal{J}_R}{d}.
 \end{aligned}
 \tag{3.37}$$

Note that the N'_p that enters in the formula for the inter-center separation r_{12} is always positive, so the radius always becomes small when the magnitude of N'_p grows. This reflects the fact that a supertube near a black hole can be merged into the black hole when the horizon radius of the latter becomes large enough [53–55].

Thus we can immediately fix the Q_I and consider the q_I as parameters. We simplify the analysis by assuming $N_1 = N_5$ and take $q_1 = q_2 = q$. This reduces our parameter space by one dimension and corresponds physically to restricting our attention to a system with an equal number of N_1 and N_5 branes.

Note that we have used the CFT charges N'_p and \mathcal{J}'_L above, as these are related by spectral flow to the enigmatic phase discussed in section 2.2.3 (the other charges do not flow). A very useful constraint coming from the CFT is eq. (2.13) which holds only for $\eta = 0$ (but can be flowed to any frame). In terms of the bulk charges it is

$$|\mathcal{J}_L| - |\mathcal{J}_R| = 2N_p \tag{3.38}$$

where we use the unflowed N_p and \mathcal{J}_L . Recall that we can fix conventions so that $\mathcal{J}_L > 0$, but once such conventions are chosen we still need to check the sign of \mathcal{J}_R . It follows from $\mathcal{J}_R = d r_{12}$ that the sign of \mathcal{J}_R is the same as that of d , so we cannot fix the sign of \mathcal{J}_R , as defined in (3.37), as this would over-constrain the bulk charges. However, as mentioned above, we do have the freedom to choose the axis along which we measure J_R at infinity so we can always choose an axis such that the latter is positive²³ giving $J_R = \pm \mathcal{J}_R$ with the \pm corresponding to the sign of d . Thus in the bulk we have

$$J'_L = d N'_p + \frac{q^2}{d} + m, \quad J_R = \begin{cases} \frac{q^2}{d} - d N'_p & (d > 0) \\ d N'_p - \frac{q^2}{d} & (d < 0) \end{cases}, \tag{3.39}$$

$$J_L - J_R = 2N_p. \tag{3.40}$$

Hence we need to consider separately the supertubes with $d < 0$ and $d > 0$. Let us also recall that the spectral-flowed charges are

$$J'_L = J_L + 2\eta N, \quad N'_p = N_p + \eta J_L + \eta^2 N. \tag{3.41}$$

3.3.1 Spectral Window

Let us examine the configuration above and attempt to constrain it as best we can by the various no-CTC conditions. We first note that if $Z_I = 0$ for any I then the condition (3.13)

²³Equivalently we can always flip the orientations of the centers in the bulk so that $\langle \Gamma_1, \Gamma_2 \rangle > 0$ by interchanging $\Gamma_1 \leftrightarrow \Gamma_2$.

is violated and we generate CTC's. This necessarily happens if q and Q have different signs since then Z_1 and Z_2 will become zero at some point (this argument is insensitive to having $N_1 = N_5$). Thus we must have

$$0 \leq q < N_5 = \sqrt{N}. \tag{3.42}$$

Likewise, positivity of r_{12} requires $q^2 \geq d^2 N'_p$, and hence

$$d^2(N_p + \eta J_L + \eta^2 N) \leq q^2 \leq N \tag{3.43}$$

and we recall from the CFT discussion that we are interested in the range of charges

$$2N_p \leq J_L \leq N + N_p. \tag{3.44}$$

From the condition $d^2 N'_p < N$ it is not hard to see that the spectral flow parameter, η , is constrained to be between 0 and -1 . As noted before η need not be integral so in principle any value $-1 \leq \eta \leq 0$ is allowed but it is possible to check, numerically, that the entropy is always maximized for $\eta = 0, -1$ so from now on we will allow only these two possibilities.

Let us review this logic. In section 3.2.3 we showed that an arbitrary two-center configuration with one smooth center can be flowed to a BMPV plus a supertube. By construction this flow does not change the character of either center (the black hole remains a black hole or a black ring, and the smooth D6 center remains a smooth D6 center or is transformed into a smooth “supertube” center). In particular, the value of the black hole or black ring entropy remains the same, although its dependence on the charges changes.

Since it is always possible to flow to a BMPV plus supertube, there exists some value of η which flows the putative bulk dual of the CFT phase to a supertube plus BMPV configuration. We analyze the CFT constraints on the charges in the flowed frame as a function of η and find they can only be satisfied for $-1 \leq \eta \leq 0$. A further numerical scan shows that the entropy is always maximized on the boundaries of this region ($\eta = 0, -1$). Since, by assumption, we started with a well-defined two-center configuration and spectral flow does not generate CTCs this shows that the BMPV plus supertube configuration must correspond to a spectral flow of $\eta = 0$ or $\eta = -1$ of the bulk configuration maximizing the entropy.

Note this argument did not involve any sort of entropy maximization over the set of all two-center solutions, which is notoriously difficult because of the absence of intuition about the relation between the charges of the centers and the appearance of CTC's. Rather, we maximize the entropy of a BMPV black hole surrounded by a supertube (where it is well-understood where CTC's come from) and use the charge relations given in section 2.2.3 to argue that the only possible dual bulk configuration can be a BMPV plus supertube, or its spectral flow by $\eta = -1$.

3.3.2 Entropy Maximization of a BMPV Black Hole Surrounded by a Supertube

The entropy of this system, comes from the BMPV center, and is

$$S(\Gamma_1) = 2\pi\sqrt{D(\Gamma_1)}, \tag{3.45}$$

where

$$D(\Gamma_1) = (\sqrt{N} - q)^2 N'_p - \frac{m^2}{4}. \quad (3.46)$$

It is clear that the entropy is maximized by minimizing q and m . These can be expressed in terms of the original CFT charges via

$$\begin{aligned} q^2 &= d^2(r_{12} + N_p + \eta J_L + \eta^2 N) \\ &= d(\pm J_R + d(N_p + \eta J_L + \eta^2 N)), \\ m &= J'_L \mp J_R - 2d N'_p \end{aligned} \quad (3.47)$$

where the \pm sign in the second lines corresponds to the cases $d > 0$ and $d < 0$, respectively, (and likewise the \mp in the third line) as follows from eq. (3.39). To facilitate the analysis let us simplify our notation and use variables $J_L = jN$ and $N_p = pN$ with $2p \leq j \leq 1 + p$ (and $p > 0$). We also use $J_R = J_L - 2N_p$ to arrive at

$$\begin{aligned} q^2 &= Nd(\pm(j - 2p) + d(p + \eta j + \eta^2)), \\ m &= N((1 \mp 1)j \pm 2p + 2\eta - 2d(p + \eta j + \eta^2)). \end{aligned} \quad (3.48)$$

It is not hard to see that q^2 is monotonic in $|d|$ in the regime $2p \leq j \leq 1 + p$ for any η while for m^2 this also happens for $\eta = 0, -1$. Thus it is always entropically favorable to take $|d| = 1$.

Let us combine these constraints to compute $D(\Gamma_1)$ in terms of the CFT parameters. We can restrict the four cases $\eta = 0, -1$ and $d = \pm 1$ and we find the two dominant combinations

$$\begin{aligned} D_a &= N^2 \left(1 - \sqrt{j - p}\right)^2 p, & (\eta = 0, d = 1) \\ D_b &= N^2 \left(1 - \sqrt{1 - p}\right)^2 (1 + p - j), & (\eta = -1, d = -1) \end{aligned} \quad (3.49)$$

The cross-over between the two entropies seems to occur at $j = 1$ and this will be borne out from the numerical evaluations below.

Although D_a and D_b are positive and real for $p \leq j \leq 1 + p$ (or $0 \leq j \leq 1 + p$ for D_b) this is misleading as we know the relation $J_L - J_R = 2N_p$ restricts J_L from below. In the bulk this relation simply follows from $r_{12} = J_R = J_L - 2N_p$. Thus these configurations exist only for $j > 2p$.

Let us consider the new maximal-entropy configurations we have found. For $j < 1$ the maximal entropy bulk configuration has $\eta = 0$ and is thus a BMPV plus supertube (as we did not have to flow). The charges for this configuration after maximization are found to be

$$\Gamma_{\text{bmpv}} = \{1, \{0, 0, 0\}, \{\sqrt{N} - \sqrt{J_L - N_p}, \sqrt{N} - \sqrt{J_L - N_p}, N_p\}, 0\}, \quad (3.50)$$

$$\Gamma_{\text{tube}} = \{0, \{0, 0, 1\}, \{\sqrt{J_L - N_p}, \sqrt{J_L - N_p}, 0\}, J_L - N_p\}. \quad (3.51)$$

For $j > 1$ the maximal entropy phase corresponds to a configuration which must be flowed by $\eta = -1$ to give a BMPV plus tube.

Recall that spectral flow is accomplished by a γ -transformation, but only after a g -transformation whose coefficient is fixed by the constraint that the total D6 charge after the flow be equal to 1 (3.34):

$$g^3 = -d \quad \text{followed by} \quad \gamma_3 = -1. \quad (3.52)$$

The resulting solution is a black ring in a background with non-trivial Wilson lines,²⁴ which we can undo by a further g -transformation:

$$\{g^1, g^2, g^3\} = \{-q, -q, 1\}. \quad (3.53)$$

The final solution is thus an asymptotically $AdS_3 \times S^3$ black ring:

$$\begin{aligned} \Gamma_1 &= \{0, \{\sqrt{N} - \sqrt{N - N_p}, \sqrt{N} - \sqrt{N - N_p}, 1\}, \\ &\quad \{\sqrt{N - N_p}, \sqrt{N - N_p}, 2\sqrt{N - N_p}(\sqrt{N} - \sqrt{N - N_p})\}, J_L - 2N_p\} \\ \Gamma_2 &= \{1, \{0, 0, 0\}, \{0, 0, 0\}, 0\}. \end{aligned}$$

Hence the cross-over between D_a and D_b is the cross-over between a solution describing a BMPV black hole surrounded by a supertube and a solution describing a black ring, and from now on we will refer to D_a and D_b as D_{tube} and D_{BR} . Thus, the entropy of the two-center configurations is

$$S_{\text{tube}} = 2\pi\sqrt{D_{\text{tube}}}, \quad D_{\text{tube}} = N^2 \left(1 - \sqrt{j - p}\right)^2 p, \quad (3.54)$$

$$S_{\text{BR}} = 2\pi\sqrt{D_{\text{BR}}}, \quad D_{\text{BR}} = N^2 \left(1 - \sqrt{1 - p}\right)^2 (1 + p - j). \quad (3.55)$$

3.3.3 New Phases in Supergravity

We have now established that there exist two maximal entropy configurations (with cross-over at $j = 1$) that have the same quantum numbers as the new CFT phase. Unfortunately neither of these phases has the same entropy as the CFT but interestingly they are restricted to the same regime of validity as the enigmatic CFT phase, namely $2p \leq j \leq 1 + p$. As the bulk entropy is lower than that of the CFT it seems, as expected, that unprotected states are lifting as we go to strong coupling. Surprisingly, however, our results suggest that not all states lift. The new phases we find in the bulk indicate that many states that do not contribute to the elliptic genus in fact do not lift at strong coupling. Furthermore, those are not just a small subset of the original states: the entropy of the bulk objects has the same growth with the charges as the entropy of the CFT. As mentioned before, this might be the consequence of some, as yet undiscovered, index that captures some fraction of the entropy of the enigmatic CFT phase.

In figure 12, we plot the entropy for these two-center phases, as well as that of the single-center BMPV black hole and the CFT phase to see how they compare. We plot the entropies versus j , for specific fixed values of p , namely $p = 0.2$ (left column) and $p = 0.9$ (right column). First, from the $p = 0.2$ graphs, we see that, for $j < 1$, D_{tube} dominates over D_{BR} while, for $j > 1$, D_{BR} dominates over D_{tube} . On the $j = 1$ line,

²⁴These Wilson lines correspond in four dimensions to Abelian flux on the D6 center

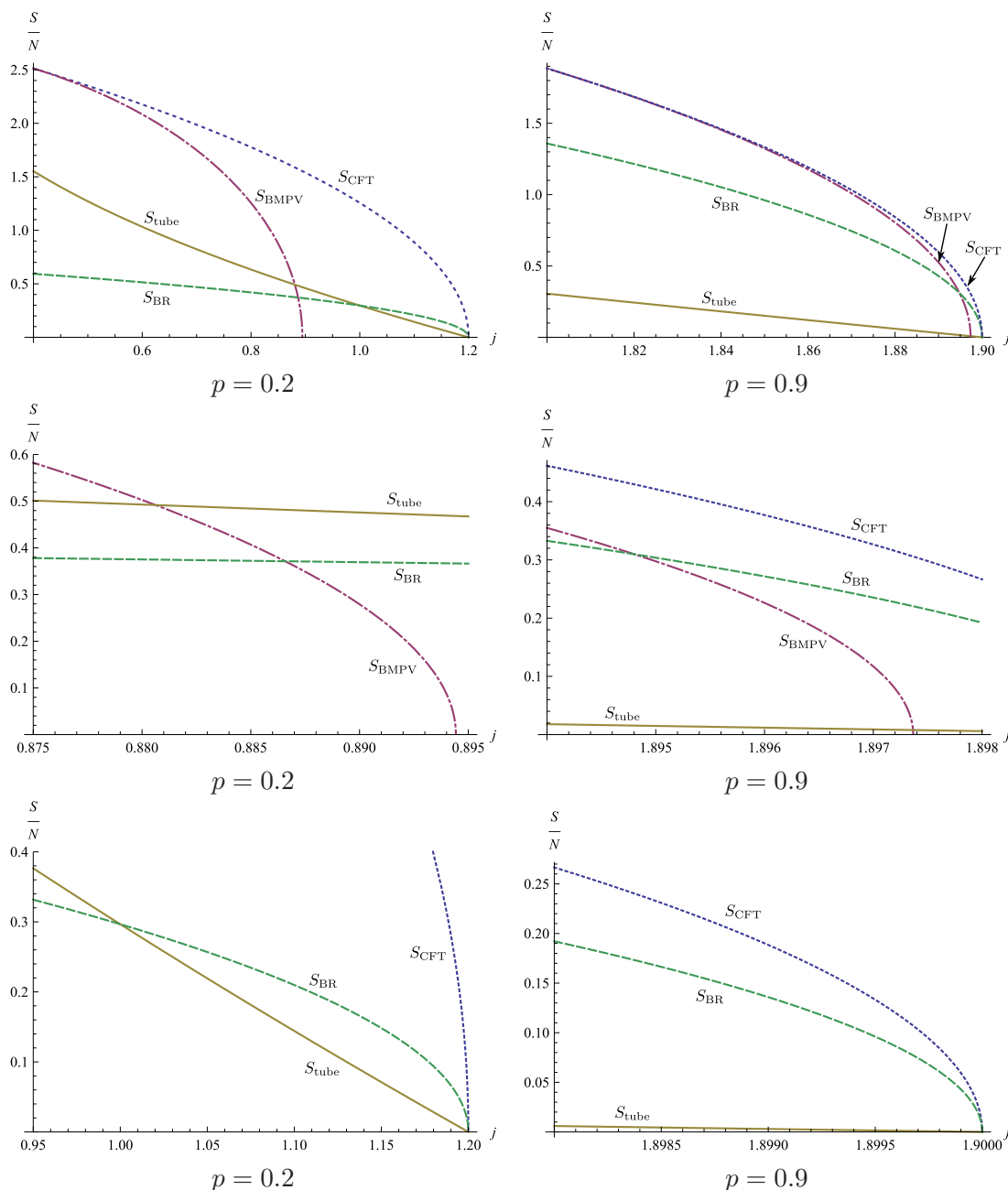


Figure 12. Plots of the various entropies. The new phases are in green (dashed), $S_{\text{BR}} = 2\pi N(1 - \sqrt{1-p})\sqrt{1+p-j}$, and brown/yellow (solid), $S_{\text{tube}} = 2\pi N(1 - \sqrt{j-p})\sqrt{p}$. For comparison we plot, in blue (dotted), the CFT entropy, $S_{\text{CFT}} = 2\pi N\sqrt{p(1+p-j)}$, and, in purple (dot-dashed), the entropy of a single-center BMPV black hole with the same charges, $S_{\text{BMPV}} = 2\pi N\sqrt{p-j^2/4}$.

the two entropies are degenerate, $D_{\text{tube}} = D_{\text{BR}}$, although the actual configurations remain different. However, because these phases exist only for $j > 2p$, if p is too large, including $p = 0.9$, the BMPV+supertube (or “BMPV+tube”) phase ceases to exist in the allowed range of j and only the black ring phase exists.

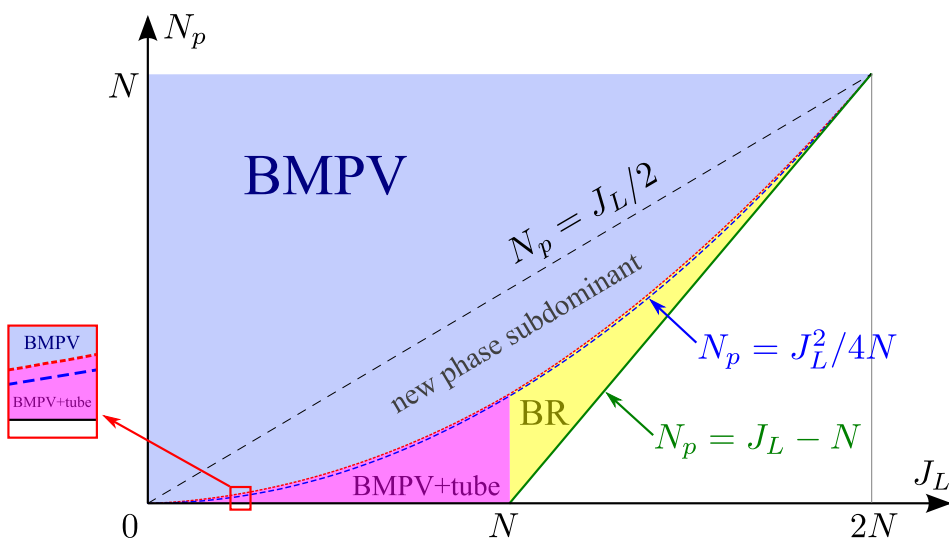


Figure 13. The bulk phase diagram. In the light blue region, the single-center BMPV black hole is dominant. In the pink and yellow regions the new phase dominates, either as a BMPV black hole surrounded by a supertube for $J_L < N$ (pink), or as a black ring for $J_L > N$ (yellow). Below the thin dashed black line and above the dotted red curve, the BMPV phase and the new phase coexist but the BMPV phase is dominant. In the narrow region between the dotted red curve and dashed blue curve, the two phases coexist and the new phase is dominant.

Next, we can ask how do the two-center entropies D_{tube} and D_{BR} compare with D_{BMPV} , the entropy of the single-center BMPV phase? For $j > 2\sqrt{p}$, which corresponds to the region below the BMPV bound $p = j^2/4$, the BMPV phase does not exist and the two-center phases are the dominant phases (although only one of them is dominant depending on $j \leq 1$ as we just discussed). On the other hand, for $j < 2\sqrt{p}$, which corresponds to the region above the BMPV bound, the two-center phase dominates over the single-center BMPV phase in a certain small range of j below the bound $j = 2\sqrt{p}$. Again, depending on the value of j , the dominant phase is either the BMPV+tube phase ($j < 1$) or the black ring phase ($j > 1$).

All these can be seen much more clearly in figure 13, where we present the phase diagram of the bulk D1-D5 system on the J_L - N_p plane (we have already presented a schematic version of this in figure 2b). Notably, even above the BMPV cosmic censorship bound $N_p = J_L^2/4N$, there is a region in which the new phase dominates over the single-center BMPV black hole. Also, the new phase is dominant in the whole region below the cosmic censorship bound where the phase of a gas of supergravity particles is subdominant.

4 Discussion

In this paper, we have carefully investigated the supersymmetric phases of the D1-D5 system, and found new phases on both sides of the AdS/CFT correspondence. The new phase in the CFT is always entropically dominant over the BMPV phase in the whole

parameter region where the two phases coexist, whereas the new phase in supergravity is dominant over the BMPV phase in a much smaller region. Below the cosmic censorship bound where the BMPV phase ceases to exist, the new phases are dominant both in the CFT as well as in supergravity.

In the CFT we found that the angular momenta of the phase that dominates the entropy satisfy the relation $J_R = J_L - 2N_p$ (eq. (2.13)). We then looked for bulk configurations that satisfy the same relation (eq. (3.39)) and obtained the phase diagram shown in figure 13.

If one relaxes this constraint, and looks instead for bulk configurations that dominate the entropy for fixed charges and J_L , one can find bulk two-center configurations (BMPV+tube and pure black ring) that have $J_R < J_L - 2N_p$ and have slightly *larger* entropy than the ones having $J_R = J_L - 2N_p$. However, the difference in entropy is small and the phase diagram is virtually unchanged from figure 13.²⁵ To avoid this unnecessary complication, we imposed the constraint $J_R = J_L - 2N_p$ in the bulk.

Thus we have found that near the boundary of the region where single-center black holes exist (the cosmic censorship bound) there appear new phases with more entropy than the single-center black hole, which can be thought of as the result of shedding of hair, or moulting, of the single center black hole. Moreover, we have seen that in different regimes of parameter space the BMPV black hole has different moulting patterns: for small J_L it sheds all its angular momentum in supertube hair, while for large J_L it sheds a hair of Gibbons-Hawking or Taub-NUT charge and becomes a black ring.

The phenomenon we find has also been seen for D4-D0 (equivalently M5-P) black holes in $\mathcal{N} = 2$ four-dimensional supergravity [11]. In both situations the new phase dominates only very close to the cosmic censorship boundary. Note that in an asymptotically-flat setting one can map the D6-D2-D0 black hole whose moulting we described here to the D4-D2-D0 black hole whose moulting was described in [11] via a combination of spectral flows, gauge transformations and 4D S -duality (equivalent to six T -dualities) [56]. This map however interchanges harmonic functions, and generically may not map asymptotically $AdS_3 \times S^3$ black holes to asymptotically $AdS_3 \times S^2$ black holes. Thus it is not immediately obvious whether the AdS moulting pattern we found here maps to the AdS moulting pattern found in [11].

4.1 A Supersymmetric Gregory-Laflamme Instability

By an analysis of the geometry similar to the one done in [57], one can show that the bulk “instability” that drives the BMPV black hole to a two-center solution can be thought of as a “supersymmetric version” of a Gregory-Laflamme instability [58]. Indeed, all the solutions we study are supersymmetric and therefore stable. However, if we make them infinitesimally non-extremal one naturally expects them to decay into more entropic configurations; thus a near-extremal BMPV black hole would decay into a near-extremal black ring or a near-extremal BMPV+supertube geometry, and would localize on the S^2 base as

²⁵A peculiar thing however is that, sufficiently inside the BMPV parabola (sufficiently away from the cosmic censorship bound), the most entropic two-center configuration has $J_R = 0$ and $r_{12} = 0$. This is a collapsing limit of the two-center solution and is singular. The entropy in this limit is smaller than that of the single-center BMPV black hole, and therefore such a configuration is never realized thermodynamically. So, this does not affect the phase diagram at all.

we explain below. This is very similar to the localization instability found for the original entropy enigma [10, 11], in which a supersymmetric black hole localizes in S^2 .

In the six-dimensional $\text{AdS}_3 \times S^3$ geometry, the original BMPV black hole is filling the entire S^3 and is pointlike in the two-dimensional spatial part of AdS_3 , which can locally be thought of as \mathbb{R}^2 . Thus the horizon topology is $S^3 \times S^1$, where S^1 is coming from fattening a pointlike object in \mathbb{R}^2 . On the other hand, the new two-center solution made of a BMPV black hole and a supertube can be thought of as a black hole which wraps the S^1 Hopf fiber of the S^3 and is pointlike in the S^2 Hopf base. It is again pointlike in the two-dimensional spatial part of the AdS_3 . Now the horizon topology is $S^1 \times S^3$, where S^3 is coming from fattening a point in the spatial part of $S^2 \times \text{AdS}_3$, which is locally \mathbb{R}^4 . Note that the tube uplifts to a smooth point on the S^3 in six dimensions (see [57], page 8).²⁶ So, in this process, the black hole localizes in the base S^2 .

It is interesting to ask why this localization occurs only in the base S^2 of the S^3 but not in the fiber S^1 , no matter how small the charges J_L, N_p are. We can argue that a complete localization in S^3 is entropically unfavorable, using an argument similar to that of [8]: Consider a small black hole localized in S^3 . For this hole to carry J_L , it must be zipping around the equator of the S^3 . Let the velocity and the rest mass of the small black hole be v and m , respectively. Its angular momentum J_L is²⁷ $J_L \sim Rmv\gamma$, while its energy is $E \sim m\gamma$, where R is the radius of S^3 and $\gamma = (1 - v^2)^{-1/2}$. If we assume that this configuration is BPS, then $N_p = ER \sim Rm\gamma$. By solving these relations for m and v , we find $m = (N_p^2 - J_L^2)^{1/2}/R$, $v = J_L/N_p$. The black hole mass m and entropy S_{small} are related to r_H by $m \sim r_H^3/G_6$ and $S_{\text{small}} \sim r_H^4/G_6$ where G_6 is the six-dimensional Newton constant. Therefore, we find $S_{\text{small}} \sim (N_p^2 - J_L^2)^{2/3} G_6^{1/3} R^{-4/3} = N(p^2 - j^2)^{2/3}$. Here, we used the relation $R \sim G_6^{1/4} N^{1/4}$ which follows from the $\text{AdS}_3/\text{CFT}_2$ dictionary. On the other hand, the entropy of the BMPV black hole is $S_{\text{BMPV}} \sim (NN_p - J_L^2/4)^{1/2} = N(p - j^2/4)^{1/2}$. Let us consider the scaling limit $N \rightarrow \infty$ with $p = N_p/N$ and $j = J_L/N$ fixed, as we have been assuming throughout the paper. We take $p, j \ll 1$ so that the radius of the BMPV black hole becomes much smaller than that of S^3 .²⁸ In order for the small black hole to exist, the reality of S_{small} requires that $p \sim j^\alpha$ with $\alpha \geq 1$ as we consider $p, j \ll 1$. In this case, $S_{\text{small}} \sim Np^{4/3} \ll S_{\text{BMPV}} \sim Np^{1/2}$ for $p \ll 1$. Namely, in the limit in which the

²⁶Some more details on the topology of the spacetime, along the lines of [57], are as follows: the five-dimensional spatial part of the spacetime can be thought of as S^1 fibered over an \mathbb{R}^4 base. The supertube worldvolume is a circle in \mathbb{R}^4 , at which the S^1 shrinks (because of the KKM dipole charge). If one considers a disk D_2 whose boundary is this circle, the S^1 fiber over the D_2 gives the S^3 . The BMPV black hole sits at the center of this D_2 . Because the S^1 fiber does not shrink there, the BMPV black hole wraps the fiber S^1 although it is pointlike in the base.

²⁷Let the S^3 be given by $\sum_{i=1}^4 (x^i)^2 = R^2$. For example, let the hole be rotating along the circle in the 1-2 plane, i.e., $(x^1)^2 + (x^2)^2 = R^2$, $x^3 = x^4 = 0$. Then the angular momentum $J^{ab} = x^a p_b - x^b p_a$ is given by $J^{12} = -J^{21} = Rmv\gamma$ with all other components vanishing. If we define J_L^i, J_R^i , $i = 1, 2, 3$ by $J_{L,R}^i = J_\pm^{i4}$, $J_\pm^{ij} = (1/2)(\tilde{J}^{ij} \pm J^{ij})$, $\tilde{J}^{ij} = (1/2)\epsilon^{ijkl} J^{kl}$, then we find $J_L^3 = -J_R^3 = -Rmv\gamma/2$. According to our definition, $J_L = 2J_L^3 = Rmv\gamma$.

²⁸From $S_{\text{BMPV}} \sim r_{\text{BMPV}}/G_3$, $R \sim G_6^{1/4} N^{1/4}$ and $G_3 \sim G_6/R^3$, it is easy to see that $r_{\text{BMPV}}/R \sim S_{\text{BMPV}}/N \sim \sqrt{p - j^2/4}$. So, $p, j \ll 1$ is sufficient for the radius of the BMPV black hole, r_{BMPV} , to become much smaller than R .

radius of the BMPV black hole becomes much smaller than that of S^3 , a full localization in S^3 is entropically unfavorable and does not happen. What happens instead is a partial localization in the S^2 base, as we have demonstrated by constructing the explicit solution.

4.2 The New Phases in the Canonical Ensemble

Thus far, we considered the new phases in the microcanonical ensemble, fixing the conserved charges N_p and J_L . It is interesting to investigate the role of the new phases in the *canonical* ensemble.²⁹ Let us flow to the NS sector where the transition from a gas of gravitons to the BMPV phase can be regarded as a Hawking-Page phase transition. In the NS sector, the entropy formulas for the BMPV phase and the new phase of the CFT are

$$S_{\text{BMPV}}^{\text{NS}}(L_0) = 2\pi\sqrt{N\left(L_0 - \frac{N}{4}\right)}, \quad S_{\text{new}}^{\text{NS}}(L_0) = 2\pi L_0, \quad (4.1)$$

where we have set $J_L = 0$ for simplicity and have used the relation (2.3) to eliminate N_p and write the equations in terms of L_0 . If we introduce the left-moving temperature T , from the thermodynamical relation $\partial S/\partial L_0 = 1/T \equiv \beta$, we obtain

$$T_{\text{BMPV}} = \frac{1}{\pi}\sqrt{\frac{L_0}{N} - \frac{1}{4}}, \quad T_{\text{new}} = \frac{1}{2\pi}. \quad (4.2)$$

Now let us go to the canonical ensemble by defining the free energy³⁰

$$F = L_0 - \frac{N}{4} - TS. \quad (4.3)$$

We find

$$F_{\text{BMPV}}(T) = -\pi^2 NT^2, \quad F_{\text{new}} = -\frac{N}{4}. \quad (4.4)$$

Note that F_{new} is defined only for $T = 1/2\pi$.

On the other hand, the thermodynamic quantities for “thermal”³¹ AdS are given by:

$$F_{\text{tAdS}} = -\frac{N}{4}, \quad S_{\text{tAdS}} = 0, \quad (L_0)_{\text{tAdS}} = 0. \quad (4.5)$$

These simply come from $e^{-\beta F} = \text{Tr}_{\text{tAdS}}[e^{-\beta(L_0 - N/4)}] \sim e^{\beta N/4}$ because only the NS ground state contributes.

We have plotted $F(T)$ for the three phases in figure 14(a). As we increase T from $T = 0$, we have a Hawking-Page transition at $T = T_c = 1/2\pi$ where the thermal AdS phase gives way to the BMPV phase. Exactly at $T = T_c$, we can have the new phase as well. The meaning of this is clearer in the graph of $T(L_0)$ shown in figure 14(b). As we increase T from $T = 0$, we first go along the vertical axis in the thermal AdS phase. Then

²⁹We thank S. Minwalla for suggesting we consider the canonical ensemble.

³⁰Because of the shift by $-c/24 = -N/4$, the relation between the partition function and the free energy is $\text{Tr}_{\text{NS,BPS}}[e^{-\beta(L_0 - c/24)}] = e^{-\beta F}$.

³¹We have a non-vanishing left-moving temperature but the right-moving temperature vanishes. Therefore the physical temperature vanishes.

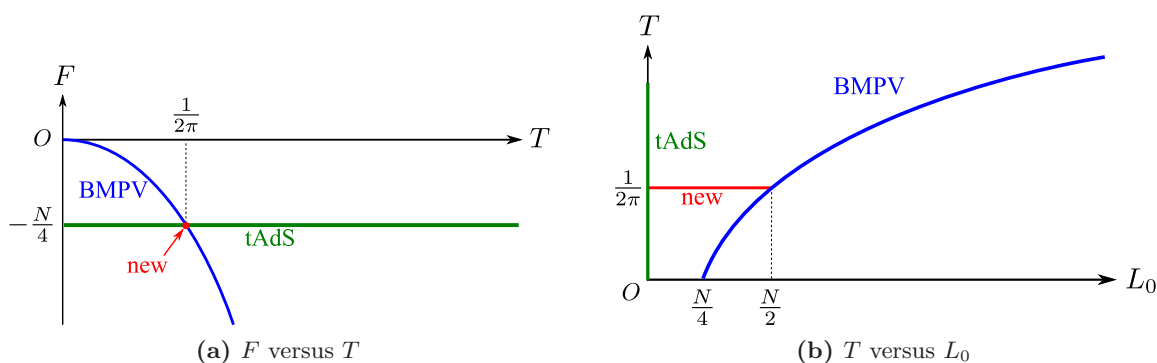


Figure 14. Thermodynamic quantities for the CFT phases in the canonical ensemble.

at $T = T_c = 1/2\pi$, we now move horizontally along the “new phase” line, and then finally reach the BMPV phase. During this horizontal motion, the temperature stays constant and the energy put into the system is used to convert the short strings into the long one. So, in the canonical ensemble, the new phase can be interpreted as the coexisting phase of the thermal AdS (short strings) and BMPV (long string) phases, much as the coexisting phase of ice and water. The difference is that ice and water coexist in the real space while the two CFT phases coexist in the space of effective strings.

We can repeat the same analysis for the bulk configuration. The entropy formulae (3.54), spectral-flowed to the NS sector, become

$$S_{new,bulk}^{NS}(L_0) = 2\pi \left(\sqrt{N} - \sqrt{N - L_0} \right) \sqrt{L_0}. \quad (4.6)$$

Note that the spectral-flowed expression for the BMPV+supertube and the black ring configurations is the same for $J_L = 0$. The temperature for this phase is

$$T_{new,bulk} = \frac{\sqrt{L_0(N - L_0)}}{2\pi(L_0 - \frac{N}{2}) + \pi\sqrt{N(N - L_0)}} \quad (4.7)$$

and the free energy is

$$F_{new,bulk} = \frac{L_0\sqrt{N}}{\sqrt{N} + 2\sqrt{N - L_0}} - \frac{N}{4}. \quad (4.8)$$

We have plotted the $F(T)$ for the BMPV, thermal AdS and the new bulk phase in figure 15(a). We have a Hawking-Page transition at $T = T_c = 1/2\pi$ where the thermal AdS gives way to the BMPV phase. The new phase exist for $\frac{1}{\sqrt{2\pi}} < T < \infty$. In figure 15(b) we plot $T(L_0)$ for the three phases. The temperature of the new phase is infinite for $L_0 = 0$ and monotonically goes down to $\frac{1}{\sqrt{2\pi}}$ at $L_0 = \frac{N}{2}$. From both these graphs we see that the new bulk phase has a negative specific heat and thus cannot be realized in the canonical ensemble even though it exists in the microcanonical ensemble.

Including $J_L \neq 0$ does not change the above qualitative picture.

4.3 Future Directions

Since our motivation has been mostly AdS/CFT-based we have focused here on a particular “moulting” of the BMPV black hole in an attempt to reproduce the CFT phase transition.

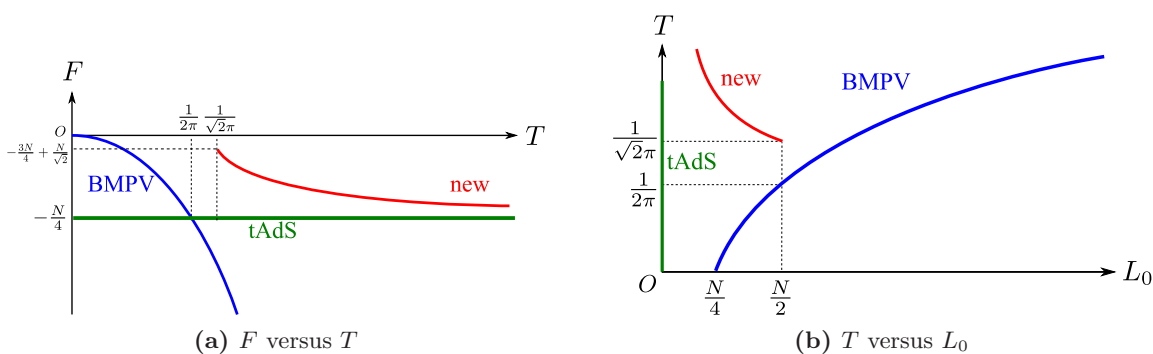


Figure 15. Thermodynamic quantities for the CFT phases in the canonical ensemble.

It is interesting to note however that an asymptotically-flat BMPV black hole can have more moulting patterns than an asymptotically-AdS one: in asymptotically-flat solutions the D1, D5, and P charges are on equal footing, and a black hole can shed either D1-D5, D1-P or D5-P supertube hair. Nevertheless, since the $AdS_3 \times S^3$ near-horizon breaks the interchange symmetry between the three charges, only the D1-D5 supertube hair remains in this limit; the other supertubes are too large and do not fit inside this near-horizon region [53].

In [24] a proposal for a CFT ensemble dual to a bulk black ring was put forward, which, modulo one phenomenological assumption about the length of the short strings, reproduces the seven-parameter entropy of the ring. The phases we discuss in this paper have short strings that have the smallest-allowed size consistent with the charges, and hence, almost by construction, have more entropy than the black ring. However, as one increases the effective coupling to move from the orbifold point to the regime where supergravity is valid, one expects the phase we constructed to lose a finite fraction of its entropy and end up describing the black ring.

There are three possible scenarios how this might happen: it may be possible that all states that have short strings of length smaller than that of [24] get uplifted, and only the states with short strings of the length of [24] or bigger survive. The second possibility is that the number of short strings stays constant as one increases the coupling, but their length changes; since the total length is constant this reduces the entropy carried by the long string, to the black ring value. The third possibility is that the phenomenological length of [24] represents the average of the lengths of the short string lengths, and that as one increases the coupling, the kind of small strings that the long string sheds changes, such that the final average is the phenomenological length.

We would also like to note that our computation of the microscopic partition function based on [41] can be straightforwardly generalized to include J_R dependence, and it would be interesting to see if this can be related to the recent results of [59] (see also [60, 61]).

In this paper, we have made a thorough search for the bulk configuration that maximizes the entropy. However, it is logically possible, although we find it unlikely, that there are some bulk configurations that have larger entropy than the ones we have been able

to find. Indeed, we made an assumption that the relevant two-center configurations have one smooth center, and the stability argument that we present in appendix C indicates that such a configuration is indeed a local maximum of the entropy; however, we could not establish that this is a global maximum, and thus it is formally possible that there are some other two-center configurations with two horizons and more entropy.

Second, we imposed a $U(1) \times U(1)$ symmetry in the bulk because the entropy-maximizing configuration in the CFT lives in a single J_R multiplet. However, as we observed above, the value of J_R that maximizes the bulk entropy is not precisely the same as the one maximizing the CFT entropy, and it is logically possible that the J_R multiplet matching does not hold; as such the maximum-entropy configuration in the bulk might break this symmetry and have more than two centers, or have some inhomogeneities.³²

These unlikely possibilities aside, our calculation shows that there exist many CFT states that are *not* protected by the elliptic genus, but that nevertheless do *not* lift at strong coupling. Furthermore, the entropy of these states is not subleading, but is of the same order of, and sometimes dominant over the entropy of the black hole. This fact either indicates the existence of a new index, or hints at a previously unthought-of dynamical mechanism that prevents the lifting of such a large number of states. We find both possibilities extremely interesting.

Acknowledgments

We thank A. Dabholkar, H. Elvang, R. Emparan, M. Guica, P. Kraus, G. Mandal, S. Minwalla, S. Murthy, K. Papadodimas and A. Virmani for helpful discussions. MS is very grateful to the ITFA, University of Amsterdam and the IPhT, CEA-Saclay where part of this work was done for hospitality. IB and MS are also grateful to the Aspen Center for Physics for hospitality, and support via the NSF grant 1066293. The work of IB and SE was supported in part by the ANR grant 08-JCJC-0001-0, and by the ERC Starting Independent Researcher Grant 240210 - String-QCD-BH. The work of BDC is supported by the ERC Advanced Grant 268088-EMERGRAV. This work is part of the research programme of the Foundation for Fundamental Research on Matter (FOM), which is part of the Netherlands Organisation for Scientific Research (NWO). The research of SE is also supported by the Netherlands Organization for Scientific Research (NWO) under a Rubicon grant.

A The Decoupling Limit

In this appendix we examine the charges and the harmonic functions that give multicenter solutions that in the IIB frame (3.18) have $AdS_3 \times S^3 / \mathbb{Z}_n$ asymptotics.³³ We take the following total charge

$$\Gamma = \{n, k^I, l_I, m\} \tag{A.1}$$

³²Much like it happens in some holographic systems where spatially inhomogeneous configurations can be thermodynamically dominant over homogeneous ones (for an incomplete list of recent work, see [62–69]).

³³A discussion of this can also be found in [53] and appendix B of [49].

and set all the constants in the harmonic functions to zero except m_0 and l_3^0 . We will generally only be concerned with the asymptotic charges but we will also need dipole charges to compute J_R asymptotically so we consider a two-center configuration with the following harmonic functions

$$V = \frac{n_1}{r_1} + \frac{n_2}{r_2}, \quad K^I = \frac{k_1^I}{r_1} + \frac{k_2^I}{r_2}, \quad (\text{A.2})$$

$$L_I = \frac{l_1^I}{r_1} + \frac{l_2^I}{r_2} + l_3^0 \delta_{I3}, \quad \tilde{M} = \frac{m_1}{r_1} + \frac{m_2}{r_2} + m_0 \quad (\text{A.3})$$

with the first center at the origin, $r_1 = |\vec{r}|$, and the second center at \vec{a} , $r_2 = |\vec{r} - \vec{a}|$. Note that this asymptotic analysis carries over straightforwardly to more centers.

We first expand the functions appearing in the metric to leading order

$$Z_1 = \frac{1}{r} \left(l_1 + \frac{k^2 k^3}{n} \right) =: \frac{N_1}{r}, \quad Z_2 = \frac{1}{r} \left(l_2 + \frac{k^1 k^3}{n} \right) =: \frac{N_5}{r} \quad (\text{A.4})$$

$$Z_3 = l_3^0 + \frac{1}{r} \left(L_3 + \frac{k_1 k_2}{n} \right) =: l_3^0 + \frac{N_P}{r}, \quad (\text{A.5})$$

from which we read off the leading terms in the IIB metric

$$ds_{\text{IIB}}^2 \sim -\frac{r}{Z_3 L} (dt + k)^2 + \frac{Z_3 r}{L} (dz + A^3)^2 + \frac{nL}{r^2} dr^2 + L \left(n d\Omega_2^2 + \frac{\sigma^2}{n} \right) \quad (\text{A.6})$$

with $L = \sqrt{N_1 N_5}$ and Ω_2 the standard S^2 metric. To connect with the standard D1-D5-P metric we consider a total charge $(1, 0, l_I, 0)$ implying that $k = 0$ and $A^3 = -Z_3^{-1} (dt + k)$ and then redefine

$$z = x_5 + \tau, \quad 2t - l_3^0 z = \tau - x_5, \quad r = \rho^2 \quad (\text{A.7})$$

putting the metric in the form

$$\frac{ds_{\text{IIB}}^2}{4} \sim \frac{\rho^2}{L} \left[-d\tau^2 + dx_5^2 + \frac{N_P}{\rho^2} (dx_5 + d\tau)^2 \right] + L \frac{d\rho^2}{\rho^2} + \frac{L}{4} (d\Omega_2^2 + \sigma^2) \quad (\text{A.8})$$

where the Hopf metric on S^3 now properly normalized. This justifies our identification of N_1, N_5 and N_P in (A.4)-(A.5).

To determine J_L and J_R we should reduce the metric (A.6) on S^3 and read off the corresponding v.e.v. from the normalizable mode of the relevant gauge fields. A simpler, albeit less direct, way to identify the charges is as follows. The relationship between μ and J_L (see eqn (3.23)) can be fixed by considering a single-center BMPV and relating its horizon entropy (in terms of harmonic functions) to what we expect from the CFT. This identification and normalization also follows from the behavior of μ under bulk spectral flow. In the M-theory frame (reduced to five dimensions) μ or J_L is related to the angular momentum along the ψ circle and the other angular momentum comes from the \mathbb{R}^3 base of the solutions (the asymptotic value of ω). Thus we can identify J_R as the asymptotic value of ω and the normalization is fixed with respect to the normalization of J_L (as we take both charges to be integral rather than half-integral).

B Spectral Flow

We provide, for reference, the charges of the ‘‘BMPV plus supertube’’ solution in terms of the charges of the original, generic, configuration from whence they were spectral flowed

$$\begin{aligned}
 \Gamma_1 = & \left\{ 1, \{0, 0, 0\}, \right. \\
 & \left\{ k_2 k_3 - l_1(\alpha - 1), k_1 k_3 - l_2(\alpha - 1), \right. \\
 & \left. \frac{p_3 (k_2 (k_1 p_3 + l_2) - (\alpha - 1) (l_3 p_3 + m)) - k_3 (l_3 p_3 + m) + l_1 (k_1 p_3 + l_2)}{(k_3 + p_3(\alpha - 1))^2} \right\}, \\
 & \frac{1}{k_3 + p_3(\alpha - 1)} \left[-k_3 (k_1 (2k_2 p_3 + l_1) + k_2 l_2 + (\alpha - 1) (m - l_3 p_3)) \right. \\
 & \left. \left. + (\alpha - 1) (p_3 (k_2 l_2 + m(-\alpha) + m) + l_1 (k_1 p_3 + 2l_2)) + k_3^2 l_3 \right] \right\}, \\
 \Gamma_2 = & \left\{ 0, \{0, 0, -\alpha (k_3 + p_3(\alpha - 1))\}, \right. \\
 & \left\{ \alpha (p_3 (k_2 + p_2(\alpha - 1)) + k_3 p_2 + l_1), \alpha (p_3 (k_1 + p_1(\alpha - 1)) + k_3 p_1 + l_2), 0 \right\}, \\
 & \left. - \frac{\alpha (p_3 (k_1 + p_1(\alpha - 1)) + k_3 p_1 + l_2) (p_3 (k_2 + p_2(\alpha - 1)) + k_3 p_2 + l_1)}{k_3 + p_3(\alpha - 1)} \right\}, \\
 h = & \{0, \{0, 0, 0\}, \{0, 0, 1\}, \alpha (k_3 + p_3(\alpha - 1))\}.
 \end{aligned} \tag{B.1}$$

Note, as emphasized in section 3.2.3, the fact that some entries are fractional poses no physical problem, because it is merely a result of the fractional spectral flow (3.34) that we chose to do.

C Stability analysis of two-center solution with one smooth center

In [11] a two-center solution was shown to be entropically dominant over a single center solution and it was assumed that keeping one center smooth would maximize the two-center entropy. Here we demonstrate the validity of this assumption locally in the space of charges for the two-center solutions considered in this paper, where one center is a BMPV black hole and the other is a smooth supertube. As described in the bulk of the paper we can use spectral flow to map this to a generic configuration with one smooth center, so the analysis performed here is broadly applicable.

Let us consider a general deformation of the BMPV+supertube system and focus on configurations and variations with equal D1 and D5 charges ($N_1 = N_5$) and equal d1 and

d5 dipole charges:

$$\begin{aligned}\Gamma_{\text{bmpv}} &= \{1, \{0, 0, 0\}, \{Q, Q, Q_3\}, m\}, \\ \Gamma_{\text{tube}} &= \{0, \{d, d, d_3\}, \{q, q, q_3\}, m'\}, \\ h &= \{0, \{0, 0, 0\}, \{0, 0, 1\}, -d_3\}.\end{aligned}\tag{C.1}$$

The equality of the charges is a simplifying assumption but should not be essential. Variations of the BMPV D4 charges can be undone by gauge transformation so the form above captures the most general (continuous) deformation. Note also that the D6 charges must remain integer in order for the background to be regular.

We parameterize the charges as

$$q = a_0 + a_1\lambda + a_2\lambda^2 + \dots, \quad q_3 = b_1\lambda + b_2\lambda^2 + \dots \tag{C.2}$$

$$d = c_1\lambda + c_2\lambda^2 + \dots, \quad d_3 = 1 \tag{C.3}$$

where we have also imposed the integrality of d_3 (which corresponds to a KK dipole charge and must be integer if the background is to be regular). The other charges can be fixed in terms of the CFT charges J_L , J_R , N and N_p and the above. We take the CFT charges to be fixed but unconstrained (we do impose the unitarity bound $J_L < N + N_p$ but this should hold for any state).

Note that a_0 is related to m' at lowest order via $m' = a_0^2 + \mathcal{O}(\lambda)$ so that to zeroth order in λ the second center is indeed a supertube. The no-CTC condition implies the q_i and Q_i must have the same sign (to leading order) so $b_1 \geq 0$ and $0 \leq a_0 \leq N_1$.

To get more constraints we consider the entropies of the two centers. To leading order the square of the entropy, $D(\Gamma_{\text{tube}})$, (see eqn (3.11)), is never positive

$$D(\Gamma_{\text{tube}}) \sim -\frac{1}{4}(b_1 - 2a_0c_1)^2\lambda^2 + \dots \tag{C.4}$$

so we must take $c_1 = b_1/2a_0$. Imposing this allows us to simplify the next non-vanishing term

$$D(\Gamma_{\text{tube}}) \sim \frac{b_1^2(2a_0(a_0a_1 + b_1) - b_1N_1)}{4a_0^3}\lambda^3 + \dots \tag{C.5}$$

whose positivity requires

$$2xa_0^2 + 2a_0 - N_1 \geq 0 \tag{C.6}$$

where we have defined $x \equiv a_1/b_1$.

Next we turn to the square of the BMPV entropy, $D(\Gamma_{\text{BMPV}})$. To zeroth order this is a quartic polynomial in a_0

$$\frac{1}{4}(-a_0^4 + 2a_0^2J_L + 2a_0^2N_P - 8a_0N_1N_P + 2J_LN_P - J_L^2 - N_P^2 + 4N_1^2N_P) \tag{C.7}$$

while its leading deformation is $\mathcal{O}(\lambda)$ and has the following form

$$\frac{b_1(a_0 - N_1)(a_0(2xN_P + N_1) - J_L + 2N_P)}{a_0}\lambda. \tag{C.8}$$

In order for the deformation to increase the entropy the expression (C.8) must be positive (the entropy contribution from the second, deformed tube, center is subleading) which gives

$$2a_0xN_P + a_0N_1 - J_L + 2N_P \leq 0. \tag{C.9}$$

Combining this with (C.6) yields upper and lower bounds on x which are only compatible when

$$a_0^2N_1 - a_0J_L + N_1N_P \leq 0. \tag{C.10}$$

Thus a_0 is constrained to lie between the roots of this polynomial.

On the other hand (C.7) is a quartic polynomial in a_0 which must be positive for the leading entropy to be real. One then checks that positivity of (C.7) is not compatible with (C.10). It then follows that any deformation that increases the entropy also generates a CTC so the BMPV plus tube center is (locally) entropically stable.

D Why the “enigmatic states” do not contribute to the elliptic genus

From a numerical analysis in section 2.3 we saw that the enigmatic phase does not contribute to the elliptic genus while the BMPV phase does. In this appendix we will give an explanation of why the particular states we consider, namely the ones of the form of a long string with excitations on it plus multiple short strings of length one, do not contribute to the elliptic genus.

For the enigmatic phase, we determined the number of short strings, l , by maximizing the entropy; this number l is given in eq. (2.10). However, other states with different number of short strings, call it $l + \delta l$, also contribute to the elliptic genus. Here, let us sum up the contributions from the states with different values of δl , and show that the sum vanishes, because of the alternating signs for bosonic and fermionic states.

If we change the number of length-one short strings by δl , the total J_L remains the same but $J_R = J_L - 2N_p + \delta l$ and it can be seen that the entropy is

$$S_{\delta l} = S_l - \frac{\delta l^2}{8S_l}. \tag{D.1}$$

This approximation is valid for $\delta l \ll S_l$. For the enigmatic phase $S_l \sim N$ and this bound is $\delta l \ll N$. Thus the elliptic genus (2.22) is given approximately by

$$\begin{aligned} \chi_{EG;enigma} &\approx e^{S_{enigma}} \sum_{\delta l=-\infty}^{\infty} (-1)^{\delta l} e^{-\frac{\delta l^2}{8S_{enigma}}} \\ &= e^{S_{enigma}} \vartheta_4 \left(0, e^{-\frac{1}{4S_{enigma}}} \right) \end{aligned} \tag{D.2}$$

where we have ignored the error in summing from $-\infty$ to ∞ instead of $-N$ to N as it goes to zero when $N \rightarrow \infty$.

We can now use modular transformation properties of theta functions to write this as

$$\chi_{EG;enigma} \approx e^{S_{enigma}} \sqrt{8\pi S_{enigma}} \vartheta_2 \left(0, e^{-16\pi^2 S_{enigma}} \right), \tag{D.3}$$

and it is easy to see that this vanishes for $S_{enigma} \rightarrow \infty$. Thus these states do not contribute to the elliptic genus.

E Units and conventions

Newton's constant in D spacetime dimensions is related to the D -dimensional Planck length as

$$G_D = (2\pi)^{D-3}(\ell_D)^{D-2}. \tag{E.1}$$

The tensions of the extended objects in string and M-theory are:

$$\begin{aligned} T_{F1} &= \frac{1}{2\pi l_s^2}, & T_{Dp} &= \frac{1}{g_s(2\pi)^p(l_s)^{p+1}}, & T_{NS5} &= \frac{1}{g_s^2(2\pi)^5(l_s)^6}, \\ T_{M2} &= \frac{1}{(2\pi)^2(l_{11})^3}, & T_{M5} &= \frac{1}{(2\pi)^5(l_{11})^6}, \end{aligned} \tag{E.2}$$

where g_s is the string coupling constant and l_s is the string length. The eleven-dimensional Planck length is related to these as

$$l_{11} = g_s^{1/3} l_s. \tag{E.3}$$

In a compactification of M-theory along a circle of radius R_{11} we get

$$R_{11} = g_s l_s. \tag{E.4}$$

In a T^6 compactification of M-theory, where the radius of each torus circle is R_5, \dots, R_{10} , the five-dimensional Planck length is related to the eleven-dimensional Planck length as

$$G_5 = \frac{G_{11}}{\text{vol}(T^6)} = \frac{G_{11}}{(2\pi)^6 R_5 R_6 R_7 R_8 R_9 R_{10}} = \frac{\pi}{4} \frac{(l_{11})^9}{R_5 R_6 R_7 R_8 R_9 R_{10}}. \tag{E.5}$$

The relation between the integer charges counting the number of M2 and M5 branes, N_I and n^I , and the physical charges of the five-dimensional solution, Q_I and q^I , upon compactification of M-theory on T^6 is

$$\begin{aligned} Q_1 &= \frac{(l_{11})^6}{R_7 R_8 R_9 R_{10}} N_1, & Q_2 &= \frac{(l_{11})^6}{R_5 R_6 R_9 R_{10}} N_2, & Q_3 &= \frac{(l_{11})^6}{R_5 R_6 R_7 R_8} N_3, \\ q^1 &= \frac{(l_{11})^3}{R_5 R_6} n^1, & q^2 &= \frac{(l_{11})^3}{R_7 R_8} n^2, & q^3 &= \frac{(l_{11})^3}{R_9 R_{10}} n^3. \end{aligned} \tag{E.6}$$

In this paper we choose a system of units where all the three T^2 are of equal volume and we have

$$R_5 R_6 = R_7 R_8 = R_9 R_{10} = \frac{1}{2} l_{11}^3 = \frac{1}{2} g_s l_s^3 \tag{E.7}$$

Note that this is a numerical identity. With this choice we have

$$G_5 = 2\pi, \quad Q_I = 4N_I, \quad q^I = 2n^I. \tag{E.8}$$

Open Access. This article is distributed under the terms of the Creative Commons Attribution License which permits any use, distribution and reproduction in any medium, provided the original author(s) and source are credited.

References

- [1] S.S. Gubser, *Breaking an Abelian gauge symmetry near a black hole horizon*, *Phys. Rev. D* **78** (2008) 065034 [[arXiv:0801.2977](#)] [[INSPIRE](#)].
- [2] S.A. Hartnoll, C.P. Herzog and G.T. Horowitz, *Building a Holographic Superconductor*, *Phys. Rev. Lett.* **101** (2008) 031601 [[arXiv:0803.3295](#)] [[INSPIRE](#)].
- [3] S.A. Hartnoll, C.P. Herzog and G.T. Horowitz, *Holographic Superconductors*, *JHEP* **12** (2008) 015 [[arXiv:0810.1563](#)] [[INSPIRE](#)].
- [4] F. Denef and S.A. Hartnoll, *Landscape of superconducting membranes*, *Phys. Rev. D* **79** (2009) 126008 [[arXiv:0901.1160](#)] [[INSPIRE](#)].
- [5] S.S. Gubser, C.P. Herzog, S.S. Pufu and T. Tesileanu, *Superconductors from Superstrings*, *Phys. Rev. Lett.* **103** (2009) 141601 [[arXiv:0907.3510](#)] [[INSPIRE](#)].
- [6] J.P. Gauntlett, J. Sonner and T. Wiseman, *Holographic superconductivity in M-theory*, *Phys. Rev. Lett.* **103** (2009) 151601 [[arXiv:0907.3796](#)] [[INSPIRE](#)].
- [7] J.P. Gauntlett, J. Sonner and T. Wiseman, *Quantum Criticality and Holographic Superconductors in M-theory*, *JHEP* **02** (2010) 060 [[arXiv:0912.0512](#)] [[INSPIRE](#)].
- [8] S. Bhattacharyya, S. Minwalla and K. Papadodimas, *Small Hairy Black Holes in $AdS_5 \times S^5$* , *JHEP* **11** (2011) 035 [[arXiv:1005.1287](#)] [[INSPIRE](#)].
- [9] J.P. Gauntlett and J.B. Gutowski, *Concentric black rings*, *Phys. Rev. D* **71** (2005) 025013 [[hep-th/0408010](#)] [[INSPIRE](#)].
- [10] F. Denef and G.W. Moore, *Split states, entropy enigmas, holes and halos*, *JHEP* **11** (2011) 129 [[hep-th/0702146](#)]. 149 pages, 21 figures [[INSPIRE](#)].
- [11] J. de Boer, F. Denef, S. El-Showk, I. Messamah and D. Van den Bleeken, *Black hole bound states in $AdS_3 \times S^2$* , *JHEP* **11** (2008) 050 [[arXiv:0802.2257](#)] [[INSPIRE](#)].
- [12] J.M. Maldacena, A. Strominger and E. Witten, *Black hole entropy in M-theory*, *JHEP* **12** (1997) 002 [[hep-th/9711053](#)] [[INSPIRE](#)].
- [13] R. Minasian, G.W. Moore and D. Tsimpis, *Calabi-Yau black holes and $(0,4)$ σ -models*, *Commun. Math. Phys.* **209** (2000) 325 [[hep-th/9904217](#)] [[INSPIRE](#)].
- [14] J. Breckenridge, R.C. Myers, A. Peet and C. Vafa, *D-branes and spinning black holes*, *Phys. Lett. B* **391** (1997) 93 [[hep-th/9602065](#)] [[INSPIRE](#)].
- [15] R. Dijkgraaf, J.M. Maldacena, G.W. Moore and E.P. Verlinde, *A Black hole Farey tail*, [hep-th/0005003](#) [[INSPIRE](#)].
- [16] J. de Boer, *Large- N elliptic genus and AdS/CFT correspondence*, *JHEP* **05** (1999) 017 [[hep-th/9812240](#)] [[INSPIRE](#)].
- [17] J.M. Maldacena, G.W. Moore and A. Strominger, *Counting BPS black holes in toroidal Type II string theory*, [hep-th/9903163](#) [[INSPIRE](#)].
- [18] A. Dabholkar, M. Guica, S. Murthy and S. Nampuri, *No entropy enigmas for $N = 4$ dyons*, *JHEP* **06** (2010) 007 [[arXiv:0903.2481](#)] [[INSPIRE](#)].
- [19] T. Eguchi, H. Ooguri and Y. Tachikawa, *Notes on the $K3$ Surface and the Mathieu group M_{24}* , *Exper. Math.* **20** (2011) 91 [[arXiv:1004.0956](#)] [[INSPIRE](#)].
- [20] H. Elvang, R. Emparan, D. Mateos and H.S. Reall, *A Supersymmetric black ring*, *Phys. Rev. Lett.* **93** (2004) 211302 [[hep-th/0407065](#)] [[INSPIRE](#)].

- [21] I. Bena and N.P. Warner, *One ring to rule them all ... and in the darkness bind them?*, *Adv. Theor. Math. Phys.* **9** (2005) 667 [[hep-th/0408106](#)] [[INSPIRE](#)].
- [22] H. Elvang, R. Emparan, D. Mateos and H.S. Reall, *Supersymmetric black rings and three-charge supertubes*, *Phys. Rev. D* **71** (2005) 024033 [[hep-th/0408120](#)] [[INSPIRE](#)].
- [23] J.P. Gauntlett and J.B. Gutowski, *General concentric black rings*, *Phys. Rev. D* **71** (2005) 045002 [[hep-th/0408122](#)] [[INSPIRE](#)].
- [24] I. Bena and P. Kraus, *Microscopic description of black rings in AdS / CFT*, *JHEP* **12** (2004) 070 [[hep-th/0408186](#)] [[INSPIRE](#)].
- [25] M. Cyrier, M. Guica, D. Mateos and A. Strominger, *Microscopic entropy of the black ring*, *Phys. Rev. Lett.* **94** (2005) 191601 [[hep-th/0411187](#)] [[INSPIRE](#)].
- [26] I. Bena and N.P. Warner, *Bubbling supertubes and foaming black holes*, *Phys. Rev. D* **74** (2006) 066001 [[hep-th/0505166](#)] [[INSPIRE](#)].
- [27] P. Berglund, E.G. Gimon and T.S. Levi, *Supergravity microstates for BPS black holes and black rings*, *JHEP* **06** (2006) 007 [[hep-th/0505167](#)] [[INSPIRE](#)].
- [28] N. Iizuka and M. Shigemori, *A Note on D1 – D5-J system and 5 – D small black ring*, *JHEP* **08** (2005) 100 [[hep-th/0506215](#)] [[INSPIRE](#)].
- [29] A. Dabholkar, N. Iizuka, A. Iqbal and M. Shigemori, *Precision microstate counting of small black rings*, *Phys. Rev. Lett.* **96** (2006) 071601 [[hep-th/0511120](#)] [[INSPIRE](#)].
- [30] L.F. Alday, J. de Boer and I. Messamah, *What is the dual of a dipole?*, *Nucl. Phys. B* **746** (2006) 29 [[hep-th/0511246](#)] [[INSPIRE](#)].
- [31] A. Dabholkar, N. Iizuka, A. Iqbal, A. Sen and M. Shigemori, *Spinning strings as small black rings*, *JHEP* **04** (2007) 017 [[hep-th/0611166](#)] [[INSPIRE](#)].
- [32] M. Shigemori, *The Phases of D1-D5 CFT — Towards Understanding Black Ring Microscopics*, talk given at Massachusetts Institute of Technology, 10 October 2006.
- [33] J.R. David, G. Mandal and S.R. Wadia, *Microscopic formulation of black holes in string theory*, *Phys. Rept.* **369** (2002) 549 [[hep-th/0203048](#)] [[INSPIRE](#)].
- [34] S.G. Avery, B.D. Chowdhury and S.D. Mathur, *Deforming the D1D5 CFT away from the orbifold point*, *JHEP* **06** (2010) 031 [[arXiv:1002.3132](#)] [[INSPIRE](#)].
- [35] S.G. Avery, B.D. Chowdhury and S.D. Mathur, *Excitations in the deformed D1D5 CFT*, *JHEP* **06** (2010) 032 [[arXiv:1003.2746](#)] [[INSPIRE](#)].
- [36] S.G. Avery and B.D. Chowdhury, *Intertwining Relations for the Deformed D1D5 CFT*, *JHEP* **05** (2011) 025 [[arXiv:1007.2202](#)] [[INSPIRE](#)].
- [37] A. Schwimmer and N. Seiberg, *Comments on the $N = 2$, $N = 3$, $N = 4$ Superconformal Algebras in Two-Dimensions*, *Phys. Lett. B* **184** (1987) 191 [[INSPIRE](#)].
- [38] V. Balasubramanian, J. de Boer, E. Keski-Vakkuri and S.F. Ross, *Supersymmetric conical defects: Towards a string theoretic description of black hole formation*, *Phys. Rev. D* **64** (2001) 064011 [[hep-th/0011217](#)] [[INSPIRE](#)].
- [39] J.M. Maldacena and L. Maoz, *Desingularization by rotation*, *JHEP* **12** (2002) 055 [[hep-th/0012025](#)] [[INSPIRE](#)].
- [40] S.D. Mathur, *The Quantum structure of black holes*, *Class. Quant. Grav.* **23** (2006) R115 [[hep-th/0510180](#)] [[INSPIRE](#)].

- [41] T. Eguchi, H. Ooguri, A. Taormina and S.-K. Yang, *Superconformal Algebras and String Compactification on Manifolds with $SU(N)$ Holonomy*, *Nucl. Phys. B* **315** (1989) 193 [[INSPIRE](#)].
- [42] T. Kawai, Y. Yamada and S.-K. Yang, *Elliptic genera and $N = 2$ superconformal field theory*, *Nucl. Phys. B* **414** (1994) 191 [[hep-th/9306096](#)] [[INSPIRE](#)].
- [43] R. Dijkgraaf, G.W. Moore, E.P. Verlinde and H.L. Verlinde, *Elliptic genera of symmetric products and second quantized strings*, *Commun. Math. Phys.* **185** (1997) 197 [[hep-th/9608096](#)] [[INSPIRE](#)].
- [44] A. Castro and S. Murthy, *Corrections to the statistical entropy of five dimensional black holes*, *JHEP* **06** (2009) 024 [[arXiv:0807.0237](#)] [[INSPIRE](#)].
- [45] D. Mateos and P.K. Townsend, *Supertubes*, *Phys. Rev. Lett.* **87** (2001) 011602 [[hep-th/0103030](#)] [[INSPIRE](#)].
- [46] F. Denef, *Supergravity flows and D-brane stability*, *JHEP* **08** (2000) 050 [[hep-th/0005049](#)] [[INSPIRE](#)].
- [47] J.B. Gutowski and H.S. Reall, *General supersymmetric AdS_5 black holes*, *JHEP* **04** (2004) 048 [[hep-th/0401129](#)] [[INSPIRE](#)].
- [48] I. Bena, P. Kraus and N.P. Warner, *Black rings in Taub-NUT*, *Phys. Rev. D* **72** (2005) 084019 [[hep-th/0504142](#)] [[INSPIRE](#)].
- [49] I. Bena, N. Bobev, C. Ruef and N.P. Warner, *Supertubes in Bubbling Backgrounds: Born-Infeld Meets Supergravity*, *JHEP* **07** (2009) 106 [[arXiv:0812.2942](#)] [[INSPIRE](#)].
- [50] G. Gibbons and P. Ruback, *The Hidden Symmetries of Multicenter Metrics*, *Commun. Math. Phys.* **115** (1988) 267 [[INSPIRE](#)].
- [51] I. Bena, N. Bobev and N.P. Warner, *Spectral Flow and the Spectrum of Multi-Center Solutions*, *Phys. Rev. D* **77** (2008) 125025 [[arXiv:0803.1203](#)] [[INSPIRE](#)].
- [52] V. Balasubramanian, E.G. Gimon and T.S. Levi, *Four Dimensional Black Hole Microstates: From D-branes to Spacetime Foam*, *JHEP* **01** (2008) 056 [[hep-th/0606118](#)] [[INSPIRE](#)].
- [53] I. Bena and P. Kraus, *Three charge supertubes and black hole hair*, *Phys. Rev. D* **70** (2004) 046003 [[hep-th/0402144](#)] [[INSPIRE](#)].
- [54] D. Marolf and A. Virmani, *A Black hole instability in five dimensions?*, *JHEP* **11** (2005) 026 [[hep-th/0505044](#)] [[INSPIRE](#)].
- [55] I. Bena, C.-W. Wang and N.P. Warner, *Sliding rings and spinning holes*, *JHEP* **05** (2006) 075 [[hep-th/0512157](#)] [[INSPIRE](#)].
- [56] G. Dall'Agata, S. Giusto and C. Ruef, *U-duality and non-BPS solutions*, *JHEP* **02** (2011) 074 [[arXiv:1012.4803](#)] [[INSPIRE](#)].
- [57] O. Lunin, J.M. Maldacena and L. Maoz, *Gravity solutions for the $D1 - D5$ system with angular momentum*, [hep-th/0212210](#) [[INSPIRE](#)].
- [58] R. Gregory and R. Laflamme, *Black strings and p-branes are unstable*, *Phys. Rev. Lett.* **70** (1993) 2837 [[hep-th/9301052](#)] [[INSPIRE](#)].
- [59] J. Manschot, B. Pioline and A. Sen, *A Fixed point formula for the index of multi-centered $N = 2$ black holes*, *JHEP* **05** (2011) 057 [[arXiv:1103.1887](#)] [[INSPIRE](#)].

- [60] J. de Boer, S. El-Showk, I. Messamah and D. Van den Bleeken, *Quantizing $N = 2$ Multicenter Solutions*, *JHEP* **05** (2009) 002 [[arXiv:0807.4556](#)] [[INSPIRE](#)].
- [61] J. de Boer, S. El-Showk, I. Messamah and D. Van den Bleeken, *A Bound on the entropy of supergravity?*, *JHEP* **02** (2010) 062 [[arXiv:0906.0011](#)] [[INSPIRE](#)].
- [62] S. Nakamura, H. Ooguri and C.-S. Park, *Gravity Dual of Spatially Modulated Phase*, *Phys. Rev. D* **81** (2010) 044018 [[arXiv:0911.0679](#)] [[INSPIRE](#)].
- [63] H. Ooguri and C.-S. Park, *Holographic End-Point of Spatially Modulated Phase Transition*, *Phys. Rev. D* **82** (2010) 126001 [[arXiv:1007.3737](#)] [[INSPIRE](#)].
- [64] A. Aperis, P. Kotetes, E. Papantonopoulos, G. Siopsis, P. Skamagoulis, et al., *Holographic Charge Density Waves*, *Phys. Lett. B* **702** (2011) 181 [[arXiv:1009.6179](#)] [[INSPIRE](#)].
- [65] R. Flauger, E. Pajer and S. Papanikolaou, *A Striped Holographic Superconductor*, *Phys. Rev. D* **83** (2011) 064009 [[arXiv:1010.1775](#)] [[INSPIRE](#)].
- [66] H. Ooguri and C.-S. Park, *Spatially Modulated Phase in Holographic quark-gluon Plasma*, *Phys. Rev. Lett.* **106** (2011) 061601 [[arXiv:1011.4144](#)] [[INSPIRE](#)].
- [67] C. Bayona, K. Peeters and M. Zamaklar, *A Non-homogeneous ground state of the low-temperature Sakai-Sugimoto model*, *JHEP* **06** (2011) 092 [[arXiv:1104.2291](#)] [[INSPIRE](#)].
- [68] A. Donos and J.P. Gauntlett, *Holographic striped phases*, *JHEP* **08** (2011) 140 [[arXiv:1106.2004](#)] [[INSPIRE](#)].
- [69] S. Takeuchi, *Modulated Instability in Five-Dimensional $U(1)$ Charged AdS Black Hole with R^2 -term*, *JHEP* **01** (2012) 160 [[arXiv:1108.2064](#)] [[INSPIRE](#)].